

Gas Analysis of Phyllosilicate-Bearing Rock

and

Its Application to Mineral Exploration

by

J. Michael Palin

Submitted in Partial Fulfillment
of the the Requirements for the Degree of
Master of Science in Geology

New Mexico Institute of Mining and Technology

Socorro, New Mexico

November, 1983

ABSTRACT

Samples of phyllosilicate minerals and phyllosilicate-bearing rocks release water vapor and small amounts of carbon, sulfur, and nitrogen gases when heated to 1100 degrees C in vacuum. Separation and mass spectrometric analysis of the gases indicates they are composed of 80-100 mole % H₂O* (defined as H₂O + H₂), 0-15 mole% C, 0-10 mole % S, and minor nitrogen. Thermal release patterns confirm that H₂O* is from structural hydroxyl in the phyllosilicates. The carbon and sulfur gases appear to be from carbon and sulfur volatiles contained in the phyllosilicates. This suggests that phyllosilicate minerals retain carbon and sulfur volatile species from coexisting fluids.

Analyses of biotite, chlorite, and muscovite (sericite) mineral samples show that phyllosilicates from hydrothermal environments have double to triple the carbon and sulfur volatile contents of phyllosilicates from igneous and metamorphic environments. Analyses of altered, phyllosilicate-bearing rock samples from the porphyry copper deposits of Bingham, Utah and Copper Flat, New Mexico show that gas compositions are related to the alteration and mineralization characteristics of the sample. Samples associated with main-stage potassic alteration and copper mineralization have $(C + S)/(H_2O^* + C + S)$ ratios greater than 0.07, whereas fresh samples or those associated with late-stage alteration have $(C + S)/(H_2O^* + C + S)$ ratios less

less than 0.07.

The gas data indicate that phyllosilicates retain the highest levels of carbon and sulfur volatile species during the main-stage of hydrothermal activity in porphyry copper systems. Contouring of $(C + S)/(H_2O^* + C + S)$ ratios of samples from within the quartz monzonite stock at the Copper Flat deposit produces a pattern similar to that for copper mineralization. Thus, although further study is required, the results indicate that gas analysis of phyllosilicate-bearing rock may be a useful tool in exploration for hydrothermal mineral deposits.

TABLE OF CONTENTS

	page
ABSTRACT	ii
TABLE OF CONTENTS	iv
LIST OF FIGURES	vi
LIST OF TABLES	vii
ACKNOWLEDGEMENTS	viii
INTRODUCTION	
Statement of Problem	1
Previous Work	2
Method of Investigation	3
ANALYTICAL TECHNIQUE	
Sample Preparation	5
Analytical System	5
Procedure	7
Gas Composition Calculation	9
Uncertainty in the Analyses	10
BACKGROUND GEOLOGY	
Bingham Mine, Utah	12
Geology	12
Alteration and Mineralization	13
Copper Flat Mine, New Mexico	16
Geology	16
Alteration and Mineralization	19

ANALYTICAL RESULTS

Introduction	24
Phyllosilicate Mineral Samples	
Sample Descriptions	24
Gas Analyses	25
Phyllosilicate-Bearing Rock Samples	31
Bingham Mine Samples	
Sample Descriptions	34
Gas Analyses	35
Copper Flat Mine Samples	
Sample Descriptions	40
Gas Analyses	41
DISCUSSION	
Interpretation of the Gas Data	47
Application to Mineral Exploration	51
Suggestions for Further Study	53
SUMMARY AND CONCLUSIONS	54
REFERENCES	56
APPENDIX A: Definitions and Terminology	63
APPENDIX B: Analytical Errors	64
APPENDIX C: Sample Descriptions	65
APPENDIX D: Gas Analyses	72

LIST OF FIGURES

	page
Figure 1. Schematic diagram of the gas analytical system.	6
Figure 2. Geology, alteration, mineralization, and sample locations at the Bingham Mine, Utah.	15
Figure 3. Location map of the Copper Flat Mine, New Mexico.	17
Figure 4. Geology, alteration, mineralization, and sample locations at the Copper Flat Mine, New Mexico.	23
Figure 5. H ₂ O*-C-S diagram with gas compositions of phyllosilicate mineral samples.	27
Figure 6. Carbon verses H ₂ O contents of phyllosilicate mineral samples.	28
Figure 7. Sulfur verses H ₂ O contents of phyllosilicate mineral samples.	29
Figure 8. Thermal gas release patterns for samples of biotite, chlorite, and muscovite.	30
Figure 9. Observed and calculated thermal H ₂ O* release patterns for three phyllosilicate-bearing rock samples.	32
Figure 10. H ₂ O*-C-S diagram with gas compositions of Bingham Mine samples.	37
Figure 11. Distribution of Type I and Type II samples at the Bingham Mine.	39
Figure 12. H ₂ O*-C-S diagram with gas compositions of Copper Flat Mine samples.	44
Figure 13. Distribution of Type I and Type II samples at the Copper Flat Mine.	46
Figure 14. Geology, alteration and mineralization, and plot of $(C + S)/(H_2O^* + C + S)$ ratios of samples at the Copper Flat Mine, New Mexico.	52

LIST OF TABLES

	page
Table 1. Replicate Gas Analyses	10
Table 2. Petrography and Gas Compositions of Phyllosilicate Mineral Samples	25
Table 3. Petrography and Gas Compositions of Bingham Mine Samples	36
Table 4. Comparison of Type I and II Samples from the Bingham Mine	38
Table 5. Petrography and Gas Compositions of Copper Flat Mine Samples.	42
Table 6. Comparison of Type I and II Samples from the Copper Flat Mine.	45

ACKNOWLEDGEMENTS

I would like to thank the many people who helped make this study a reality. In particular, I thank Dr. David Norman for suggesting and encouraging the investigation; Daniel Geddert for setting up computer control of the mass spectrometer; and Carl Bernhardt, Eric Bigelow, and Robert Smith for many hours of discussion concerning analytical methods. Special thanks to the Geology Department of the Utah Copper Division of Kennecott Copper for providing samples from the Bingham Mine, and to Quintana Minerals for access to the Copper Flat Mine. I appreciate Drs. Andrew Campbell, David Norman, and James Robertson for serving on my thesis committee.

Funding for this study was provided by Office of Surface Mining, U.S. Department of Interior grant # G5104024.

INTRODUCTION

Statement of Problem

Exploration for mineral deposits is a task which has become increasingly difficult. It is a problem which often reduces to finding clues to mineralization rather than to mineralization itself. Rock alteration patterns and trace element halos are exploration methods which are presently being used to locate areas of potential hydrothermal mineralization. This investigation deals with the analysis of gases released from phyllosilicate-bearing rock and the potential this technique has in mineral exploration.

The basic hypothesis of this study is that volatile species in hydrothermal fluids are retained by phyllosilicate minerals in altered rock, and are released as gases during thermal decrepitation of samples in the laboratory. The volatile composition of hydrothermal fluids and, according to this hypothesis, coexisting phyllosilicates may be sensitive indicators of changing physiochemical conditions in a hydrothermal system, some of which are responsible for mineral deposition. If this is the case, variations in the gas compositions of phyllosilicate minerals and phyllosilicate-bearing rocks may be useful in locating areas of hydrothermal mineralization in terrains where other exploration methods are not effective.

Previous Work

Many studies have identified volatile components in minerals. Structural substitution of chlorine, fluorine, and NH_3^+ occur in several mineral types, including the phyllosilicates (Evans, 1969; Munoz and Ludington, 1974; Nash, 1976; Honma and Itihara, 1981). Foster (1964) and Banks (1973, 1982) measured sulfur in biotite and chlorite. In work similar to that of this study, Norman (1977) reported the release of CO_2 and H_2S from chlorite, sericite, and kaolinite. During analysis of volatiles in amphiboles using an electron microprobe and high-temperature mass spectrometer, Garcia and others (1980) found CO_2 and sulfur in addition to H_2O , chlorine, and fluorine. The mechanism by which these volatiles are retained in the minerals is not definitively known. Possibilities include micro-fluid inclusions (Piperov and Penchev, 1973; Garcia, et al, 1980), atomic species (Freund, et al., 1980), complex ions (Lovering and Widdowson, 1968; Mysen, et al., 1976), or gas species (Mercer, 1967).

Analysis of volatiles in rocks was done by Shepherd (1938) as an extension of an investigation of volcanic gases. Samples of rhyolitic glass, andesitic and basaltic lava, and various plutonic rocks were heated in vacuum and the gases released reported. He noted that volatile contents of altered samples were several times greater than those of fresh rock. Sheridan and Moore (1981) measured the carbon,

sulfur, and nitrogen contents of the rhyolitic Bishop Tuff. They found an enrichment of carbon and sulfur in zones of fumarolic alteration.

Limited effort has been directed at the application of these types of analyses in mineral exploration. A Russian investigation of copper-molybdenum deposits found higher levels of H₂S around skarn mineralization than with vein or disseminated mineralization, and high CO₂ concentrated in "zones of tectonic activity" (Elinson, 1970). Boyle (1979) noted the association of CH₄, CO₂, and H₂S with several Canadian lode gold deposits. In both of these cases, however, no analytical details were given. Increasing attention has been given to detection of anomalous levels of carbon and sulfur gases in soils over oxidizing sulfide deposits in a variety of geologic and climatic environments (Hinkle and Kantor, 1978; Lovell, et al., 1980; Taylor, et al., 1982). No consistently conclusive results have been obtained, however.

Method of Investigation

The goals of this study were to: 1) develop a technique for analyzing gases from phyllosilicate-bearing rock samples, 2) examine the relationships of gas data to the geology and patterns of alteration and mineralization at two hydrothermal mineral deposits, and 3) evaluate the potential of using gas analyses in mineral exploration.

The first part of the study was approached by modifying an analytical technique for the decrepitation and analysis of fluid inclusions using mass spectrometry (Norman, 1977). Phyllosilicate mineral samples were analyzed first in order to: 1) identify the gases released upon heating, 2) insure that these gases were not the result of the thermal breakdown of mineral contaminants, and 3) determine the relationship between gas content and sample occurrence. Phyllosilicate-bearing rock samples were then analyzed in order to determine whether the technique used for the mineral samples could be applied to rock samples.

The second and third parts of the investigation involved case studies at the porphyry copper deposits of Bingham, Utah and Copper Flat, New Mexico. Rock samples were collected, petrographically examined, and analyzed. The data was compared with available geologic information for the two deposits in order to: 1) relate the gas analyses to the geology, alteration, and mineralization at the deposits and 2) evaluate the potential of using the gas analysis technique in mineral exploration.

ANALYTICAL TECHNIQUE

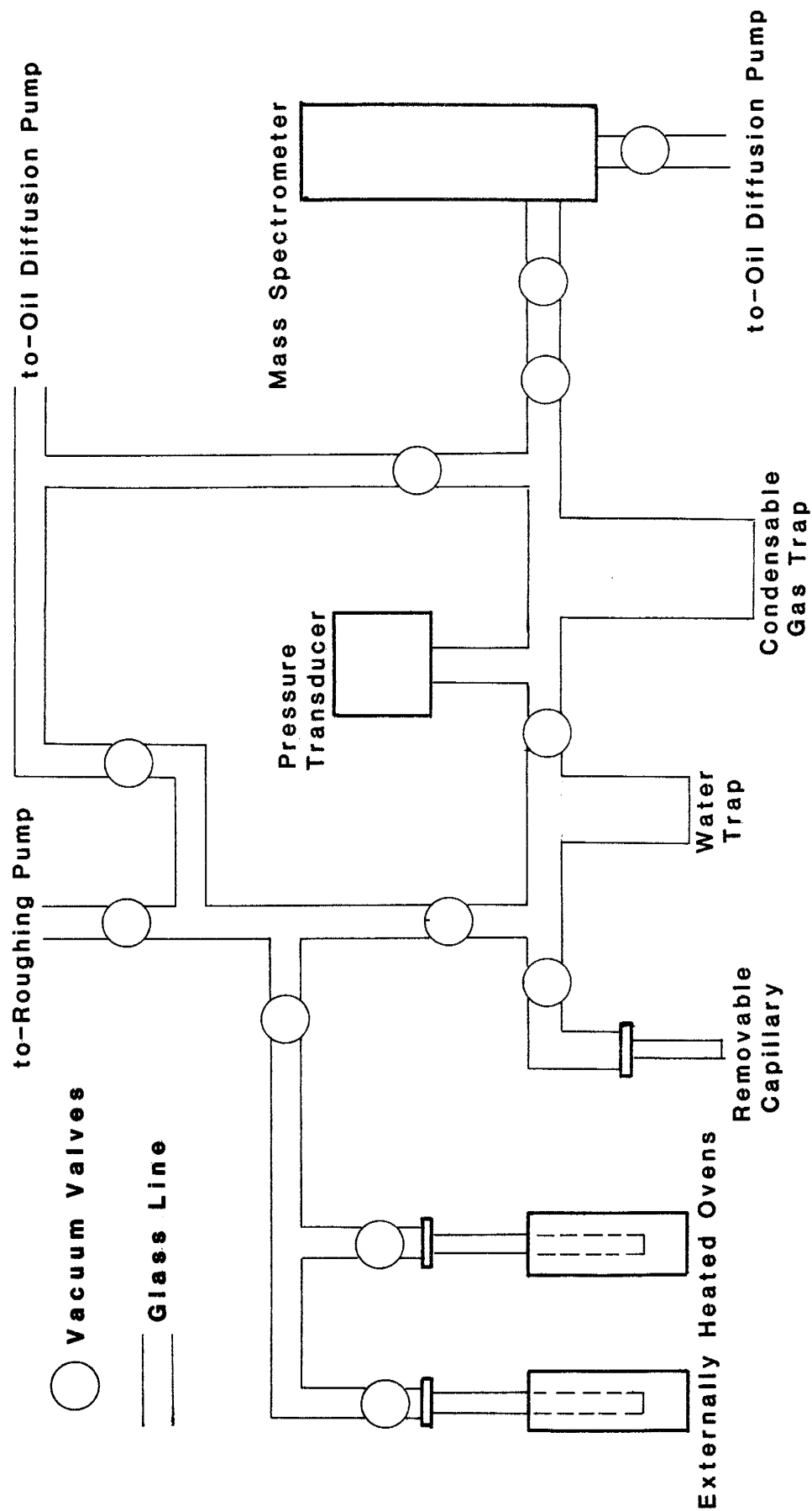
Sample Preparation

Mineral and rock samples are pulverized, hand-picked, ground to -70 to +160 mesh, and rinsed with distilled water. Sulfide minerals are separated using heavy liquids, and sulfate and carbonate minerals removed by treatment with warm dilute HCl. After multiple rinsing with distilled water, the powders are oven dried at 125 degrees C. Initially, samples are examined for impurities using a scanning electron microscope equipped with an energy dispersive detector.

Analytical System

The analytical system of this study consists of two externally heated quartz furnaces for thermally releasing gases from samples, a gas separation line for dividing gas mixtures, and a mass spectrometer for analyzing the composition of gases (Fig. 1). The sample furnaces are 35 cm long quartz tubes which are connected to the gas separation line with Cajon Ultra-Torr adaptors. The quartz tubes are heated externally by resistance ovens. Temperature is regulated through a proportional temperature controller using a chromel/alumel thermocouple. The operating limit for the furnaces is approximately 1200 degrees C.

Figure 1. Schematic diagram of the analytical system
used in this study.



The gas separation line can be evacuated to 10^{-7} torr using an oil diffusion pump. Pressures of gas samples are measured by a MKS Baratron 221AHS absolute pressure transducer (capacitance manometer). The line leads into a Leybold-Heraeus Inficon IQ200 quadrupole mass spectrometer controlled by a Hewlett-Packard HP-85 computer. The mass spectrometer makes measurements over a mass range of 1 to 200 AMU and a concentration range of five orders of magnitude. The unit can be evacuated to a pressure of 10^{-9} torr using an oil diffusion pump.

Procedure

Prepared samples, ranging from 50 mg to 1000 mg, are loaded into the quartz furnace. They are baked at 150 degrees C while being evacuated to a pressure less than 1×10^{-5} torr in order to remove absorbed components. The quartz furnace and gas separation line are then closed to the vacuum pumps.

Most samples are heated at 1100 degrees C for one hour and the gases released are analyzed in one step. Step-heated samples are heated for 30 minutes at 100 degree intervals from 300 degrees C to 1100 degrees C with gases analyzed after each step.

In order that mass peak interferences are minimized when gas mixtures are inlet into the mass spectrometer, the gases are separated into three portions according to boiling

point. These are: 1) water, 2) condensable gases (CO_2 , SO_2 , H_2S , NH_3 , and hydrocarbons heavier than methane), and 3) noncondensable gases (H_2 , N_2 , CO , CH_4 , O_2 , and Ar). While the sample is heated, the condensable trap is cooled with liquid nitrogen. This separates the condensable gases and water from the noncondensable gases as they are released from the sample. When heating is finished and the pressure in the gas separation line stabilizes and is recorded, the noncondensable gases are leaked into the mass spectrometer for analysis. When the analysis is completed, the gas separation line is evacuated, the liquid nitrogen is removed from the condensable trap, and the water trap is cooled with a dry ice-alcohol mixture. This procedure separates water from the condensable gases which vaporize and fill the gas separation line. When the pressure stabilizes and is recorded, the condensable gases are leaked into the mass spectrometer and analyzed. After the analysis, the remaining condensable gases are pumped out and the dry ice-alcohol mixture removed from the water trap. Water is transferred to a preweighed capillary tube by simultaneously heating the water trap and cooling the tip of the capillary with liquid nitrogen. When the transfer is completed, the capillary is sealed, removed, and weighed.

Gas Composition Calculation

The measured mass spectra for the noncondensable and condensable gases is reduced by means of a least-squares matrix solution on the HP-85 computer. This routine compares net spectra with measured fractionation patterns and sensitivities of pure gases to calculate the gas ratios in the noncondensable and condensable gas portions. The molar amounts of gas in each portion is calculated from the ideal gas law using the measured sample pressures and known volumes of the gas separation line. The number of moles of each gas is obtained by multiplying the molar quantities by the gas ratios.

The gases can be divided into four compositional groups; water (including H₂), carbon gases (CO₂, CO, CH₄, and hydrocarbons), sulfur gases (H₂S and SO₂), and nitrogen gases (N₂ and NH₃). The most abundant gas in all analyses is H₂O, followed by the carbon and sulfur gases. No chlorine or fluorine-bearing gases were detected. Because the ratio of oxidized to reduced species in each group is dependent, at least partially, on external factors (Norman and Palin, 1982), the gas compositions are best reported in terms of the relative mole proportions of H₂O* (defined as H₂O + H₂), total carbon, and total sulfur. These proportions can be graphically reported in H₂O*-C-S ternary diagrams.

Uncertainty in the Analyses

There are two sources of uncertainty in the gas analyses: 1) within-sample variance and 2) analytical error. It is critical to measure this uncertainty in order to determine the significance of differences in the data.

Within-sample variance is estimated by repeating gas analyses of samples and calculating the precision (Table 1).

TABLE 1. Replicate Gas Analyses

Sample	Chlorite (Chl 2)				Quartz Monzonite (CF 5-5)			
Run #	1	2	3	Prec.	1	2	3	Prec.
Size	80 mg	80 mg	80 mg		80 mg	80 mg	80 mg	
Gas (X 10 ⁻⁷ moles)								
H ₂ O	4460	4300	4390	±50	370	389	333	±16
H ₂	44.1	71.6	3.0	±20	1.1	1.7	1.4	±0.2
CO ₂	10.9	24.2	14.0	±3.9	39.9	24.5	25.7	±4.8
CO	-	-	-	-	24.4	34.1	27.9	±2.9
CH ₄	0.05	0.36	0.63	±0.17	0.7	0.9	0.7	±0.1
C ₂ H ₆	-	-	-	-	-	-	-	-
H ₂ S	9.0	19.3	7.2	±1.9	-	-	-	-
SO ₂	20.6	29.7	24.0	±2.7	0.22	1.0	0.74	±0.14
N ₂	0.64	1.6	1.8	±0.36	1.1	2.3	0.8	±0.6
NH ₃	1.3	4.5	2.6	±1.0	-	-	-	-
(mole %)								
H ₂ O*	99.1	98.3	99.0	±0.3	85.1	86.6	85.9	±0.4
C	0.2	0.6	0.3	±0.1	14.9	13.2	13.9	±0.5
S	0.7	1.1	0.7	±0.1	0.1	0.2	0.2	±0.1

The problem of analytical error is more difficult to quantify. Independent methods are not available to determine the accuracy of the analysis technique. Therefore, as an

estimate, the possible errors introduced during steps in the analytical procedure are considered. These can be combined to give a total analytical error of approximately 10% in the quantity of each gas species (see Appendix B). This is within the analytical precision for most of the gas species (Table 1).

In light of the above estimates of within-sample variance and analytical error, interpretation of the gas data is based on the relative proportions of H₂O*, C, and S in the gases rather than absolute amounts of individual gas species. The data symbols used in the H₂O*-C-S ternary diagrams of this study are drawn to include the estimated analytical uncertainty in the gas compositions.

BACKGROUND GEOLOGY

Bingham Mine, Utah

The Bingham Mine is a porphyry copper deposit located in the central Oquirrh Mountains 32 km southwest of Salt Lake City, Utah. The deposit has been a major source of copper, molybdenum, gold, and silver for nearly 80 years.

Geology

The oldest rocks exposed in the mine area (Fig. 2a) belong to the Pennsylvanian Butterfield Peak and Bingham Mine Formations which are composed predominantly of fine-grained quartzite interbedded with lesser amounts of calcareous sandstone and sandy limestone (Smith, 1978). These sedimentary rocks are cut by the multiphase Bingham intrusive complex. The main intrusive phases dealt with in this study are, from oldest to youngest: monzonite (granite of Bray, 1969; equigranular phase of Moore and Nash, 1974; monzonite of Smith, 1978), quartz monzonite porphyry (granite porphyry of Bray, 1969; aplitic porphyry of Moore and Nash, 1974; latite porphyry of Smith, 1978), and latite porphyry (rhyolite porphyry of Bray, 1969 and Moore and Nash, 1974; quartz latite porphyry of Smith, 1978). The dates for these rocks range from 39.8 ± 0.4 m.y. for the early, relatively quartz-poor, equigranular phases to 38.8 ± 0.4 m.y. for the

late, porphyritic phases (Warnaars, et al., 1978).

The major structural features present in the mine area are: 1) large, northwest-trending folds and northwest-trending thrust faults in the sedimentary section and 2) younger, northeast-trending, high-angle faults (Lanier, et al., 1978). The degree to which emplacement of the main monzonite phase of the Bingham stock was influenced by these structures is unclear (Moore and Nash, 1974; Lanier, et al., 1978). However, the orientations of the later quartz monzonite and latite phases suggests they were structurally controlled by the northeast-trending fault set (Einaudi, 1982).

Alteration and Mineralization

Hypogene alteration and mineralization at the Bingham mine are roughly centered around the quartz monzonite porphyry phase of the Bingham stock (Moore and Czamanske, 1973; Moore and Nash, 1974; Moore, 1978; John, 1978) (Figs. 2b and 2c). The coincidence of these patterns suggests a genetic link between hydrothermal activity the quartz monzonite porphyry (Moore, 1978; John, 1978; Einaudi, 1982).

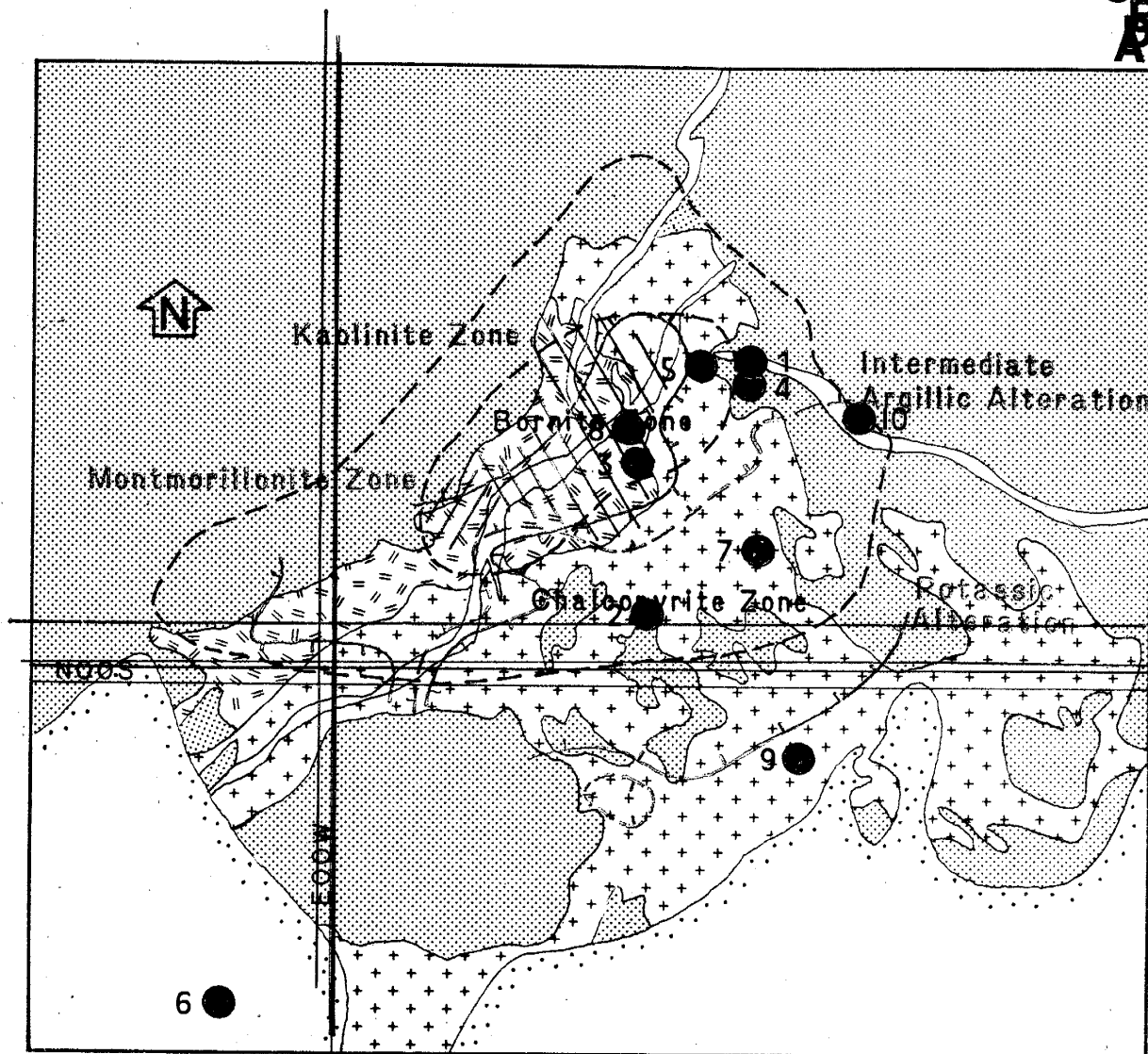
Previous studies identify three main types of alteration at the deposit. Main-stage hydrothermal activity produced potassic alteration (biotitic alteration of Moore and Nash, 1974; quartz-orthoclase-phlogopite zone of Lanier, et al., 1978) and propylitic alteration (actinolite-chlorite-epidote and calcite-chlorite-quartz zones of Lanier, et al., 1978).

An increase in the $Mg/(Mg+Fe)$ ratio of secondary biotite (phlogopite) toward the quartz monzonite porphyry indicates that it was the center of the most intense potassic alteration (Moore and Czamanske, 1974). Later hydrothermal activity produced intermediate argillic alteration (sericitic alteration of Moore and Nash, 1974; sericite-quartz zone and late argillic alteration of Lanier, et al., 1978). This late-stage alteration was probably controlled by northeast-trending faults and fractures which cut the northwest portion of the Bingham stock (Moore and Nash, 1974; Lanier, et al., 1978; Moore, 1978).

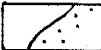
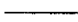

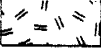


Copper mineralization is well zoned at the Bingham mine, forming a dome-shaped orebody about the quartz monzonite porphyry (John, 1978). The bornite-chalcopyrite and pyrite-chalcopyrite zones compose the main copper orebody ($>0.35\%$ Cu) and are shown in Figure 2c. The highest copper grades occur in areas of greatest fracture density in the central and northern portions of the Bingham stock (Moore and Nash, 1974). The bulk of copper mineralization is bracketed in time between the younger quartz monzonite porphyry and older latite phases of the Bingham intrusive complex (Warnaar, et al., 1978).

- Figure 2a. Simplified geologic map of the Bingham Mine area, Utah (modified from Smith, 1978).
- b. Alteration patterns (modified from Moore and Nash, 1974).
 - c. Copper orebody (from John, 1978).
 - d. Sample localities for this study.

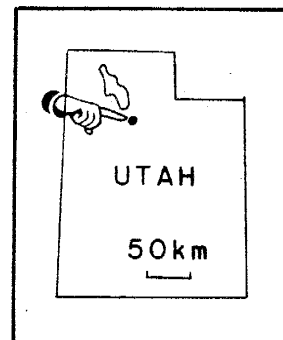
C
B
A



EXPLANATION

- | | | | |
|---|------------------------|---|----------------|
|  | Dump |  | Contact |
|  | Latites | | |
|  | Qz Monzonite | | |
|  | Monzonite | | |
|  | Bingham Mine Fm | | |

SCALE



Copper Flat Mine, New Mexico

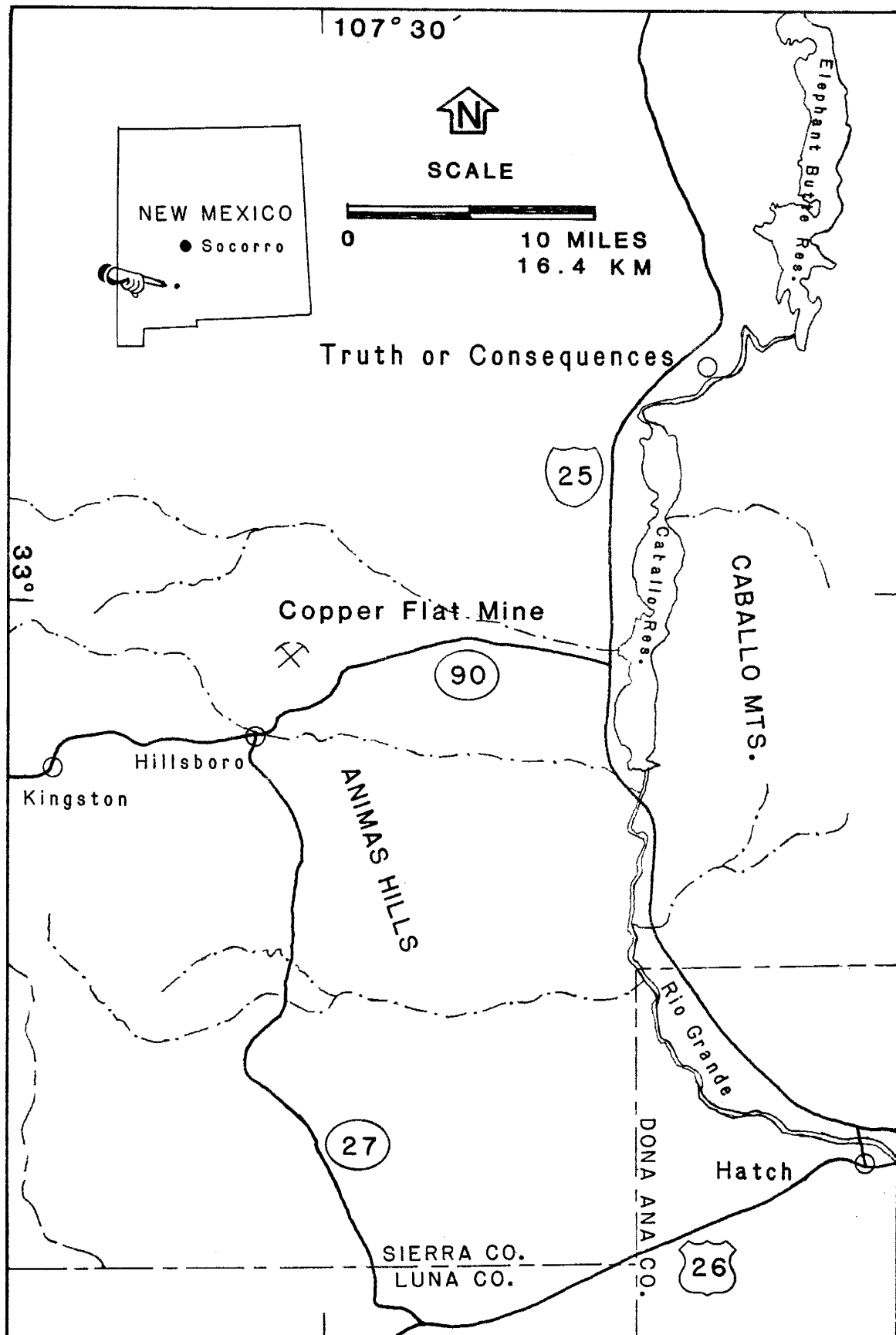
The Copper Flat porphyry copper deposit is located in the Hillsboro mining district, approximately 30 km southwest of Truth or Consequences, New Mexico (Fig. 3). From 1877 to 1974 the district recorded production of \$8.5 million, principally from Au-Ag-Cu veins and placer Au (Harley, 1934; Segerstrom and Antweiler, 1975). Exploration for a possible porphyry copper deposit was begun by Newmont Mining in 1952 in the Copper Flat basin. Further work by Bear Creek Mining in 1958-1959 established the existence of a porphyry system. Assessment was undertaken by Inspiration Consolidated Copper from 1967 to 1973. Quintana Minerals obtained the property in 1974, continued evaluation, and began development in 1980. Mineable reserves at that time consisted of 53.7 million tons of 0.42% Cu and 0.012% Mo ore with by-product Au and Ag (Dunn, 1981). The mine and mill are presently closed.

Geology

Rock Units

Although Paleozoic sediments are probably present in the subsurface (Kuellermer, 1955; Dunn, 1982), the oldest rocks exposed in the mine area are interbedded andesite breccias and flows (Fig. 4a). The Copper Flat quartz

Figure 3. Location of the Copper Flat Mine, New
Mexico.



monzonite stock cuts these volcanics and is exposed in the central part of the small Copper Flat basin. The stock is Laramide in age based on a biotite K-Ar date of 75.1 ± 2.5 m.y. (Stacey and Hedlund, 1983). Petrologic data indicate that the quartz monzonite and andesites may be comagmatic (Dunn and Fowler, 1982). Younger latite dikes cut both the stock and andesites. Basaltic dikes are also present in the mine area (not shown in Fig. 4a), and are presumably related to basalt flows which cap several local ridges.

Structure

Faults in the Hillsboro mining district (and nearby Central mining district) are predominantly northeast trending (Hedlund, 1974). This trend was a combined result of Laramide northeast-southwest directed compression, which produced a component of northwest-southeast extension (Davis, 1981), and the configuration of the Early Cretaceous Bisbee Basin in southeastern Arizona (Bilodeau, 1982).

Within the Copper Flat mine area (Fig. 4a), structures are consistent with a principle stress direction of approximately N50E (Heidrick and Titley, 1982; Cather, personal communication, 1983). These structures include three sets of faults and fractures. Those bearing N30-40E and N60-70E correspond to conjugate strain orientations, and those bearing N70W align with a left-lateral shear couple.

Alteration and Mineralization

Alteration and mineralization at the Copper Flat deposit are spatially related to a central breccia pipe within the Copper Flat stock (Fig. 4a). The breccia is potassically altered and has the highest grade mineralization. However, unlike the Bingham deposit and many other porphyry copper deposits, alteration and mineralization at the Copper Flat deposit are not well zoned (Figs. 4b and 4c).

Dunn (1982) proposes a three stage model for alteration and mineralization. Stage 1 (early-stage) consists of early pyrite and chalcopyrite mineralization in the form of disseminations and veinlets with sericitic alteration selvages. Stage 2 (main-stage) includes breccia formation and pyrite and chalcopyrite mineralization with associated potassic alteration. Stage 3 (late-stage) mineralization consists of veins of quartz \pm pyrite + chalcopyrite, quartz \pm molybdenite, and carbonate \pm sphalerite \pm galena all with selvages of sericitic alteration.

Alteration

Based on the field and petrographic observations of this study, the alteration at Copper Flat may be divided into three types: 1) potassic, 2) sericitic, and 3) propylitic. Figure 4b shows the the potassic and sericitic alteration patterns at the deposit. These outlines are based on thin

section observations and, therefore, may not be as continuous as shown.

The distribution of potassic alteration is defined by the presence of secondary potassium-feldspar and/or biotite (Fig. 4b). It is most pronounced in the breccia, where coarse-grained biotite and potassium-feldspar occur in the the matrix, and fine-grained aggregates of secondary biotite are found in quartz monzonite clasts. In the southeastern portion of the breccia, secondary biotite is not present. Fine-grained secondary biotite is disseminated in the quartz monzonite wallrock to the northwest and northeast of the breccia pipe.

The alteration of plagioclase to sericite \pm clay and mafic minerals to sericite \pm chlorite defines the distribution of sericitic alteration (Fig. 4b). This type of alteration overprints the entire Copper Flat stock to various degrees. In addition, some andesite samples exhibit abundant sericitic alteration of plagioclase in the groundmass. In all the samples of this study, sericitic alteration postdates potassic alteration.

Propylitic alteration is ubiquitous in the andesites. The characteristic assemblage is chlorite \pm epidote \pm calcite in the groundmass of flowrock. Propylitic alteration predates sericitic alteration in the andesites. However, because it is rare in the quartz monzonite, its relationship to potassic alteration cannot be established.

Mineralization

According to Dunn (1982), mineralization at Copper Flat is predominantly hypogene. The ore minerals in order of abundance are chalcopyrite, molybdenite, and minor galena and sphalerite. The occurrence of by-product Au and Ag is not known (Puipulidy, personal communication, 1981).

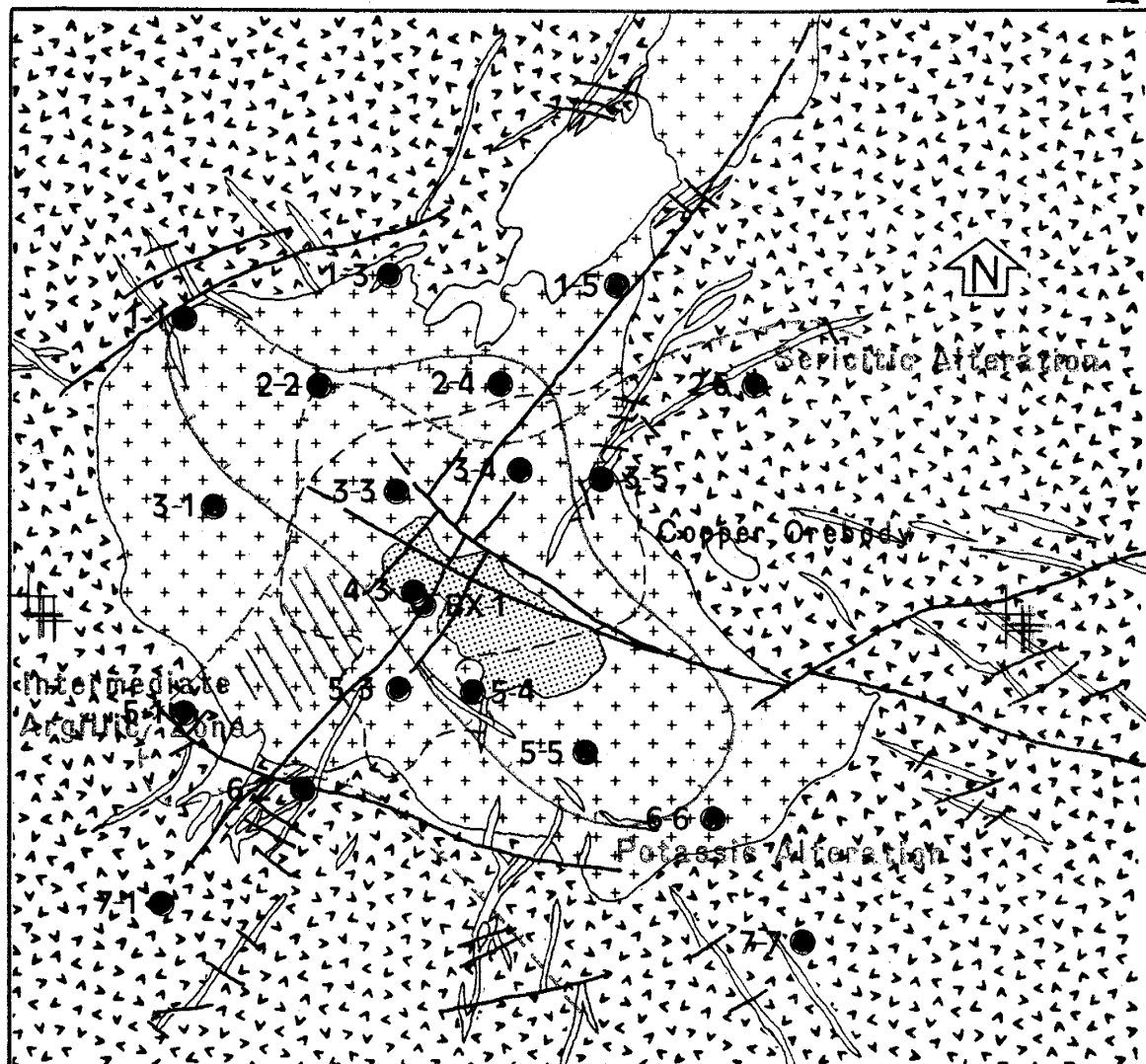
Ore grade mineralization is mainly confined to the central breccia pipe (Fig. 4c). This body is about 450 m long and 200 m wide, trends to the northwest, and dips steeply to the southwest. Mineralization is not uniformly distributed, however. The highest concentrations of copper are in the northwest portion of the pipe, with a sharp decrease in grade to the southeast (Dunn, 1982). Fluid inclusions in quartz from the breccia matrix have homogenization temperatures of 320-360 degrees C with moderate to high salinities, show evidence of boiling, and indicate a depth of formation of 1-2 km (Dunn and Fowler, 1982; Dunn, personal communication, 1982). Dunn (1982) cites this data and textures within the breccia as evidence that the breccia pipe formed as a result of retrograde boiling during the crystallization of the Copper Flat Stock (for further elaboration see Cathles, 1981, p. 445).

In the stock, the style of mineralization is different. Pyrite and chalcopyrite are present as fine-grained disseminations replacing mafic minerals or in quartz veins. The orientations of these veins correspond to the main

fault-fracture sets of the area (Dunn, 1982). Mineralization of this type occurs in the quartz monzonite stock to the northeast and west of the breccia pipe (Fig. 4c).

Figure 4a. Simplified geologic map of the Copper Flat Mine area, New Mexico (from Dunn, 1982).

- b. Alteration patterns (based on samples of this study).
- c. Copper orebody (from Dunn, 1982).
- d. Sample localities for this study.



EXPLANATION

 Breccia Pipe

 Latite

 Qz Monzonite

 Andesite

— Fault

— Contact

SCALE



ANALYTICAL RESULTS

Introduction

The analytical results of this study are presented in the following section. Phyllosilicate mineral samples were analyzed first in order to develop and test the analytical technique. Phyllosilicate-bearing rock samples were then analyzed to determine whether the technique could be extended to rock samples. After these preliminary analyses were complete, the case studies at the Bingham and Copper Flat deposits were conducted using phyllosilicate-bearing rock samples.

Phyllosilicate Mineral Samples

Sample Descriptions

Fifteen phyllosilicate mineral samples were analyzed. These samples included 6 biotites, 5 chlorites, and 4 muscovites and sericites which were selected from a wide variety of igneous, metamorphic, and hydrothermally altered rocks in order to determine the range of gas compositions of the common phyllosilicates. Medium to very coarse-grained samples were chosen in order to make mineral identification and separation easier. The descriptions of individual mineral samples are given in Appendix C.

Gas Analyses

The complete gas analysis for each of the phyllosilicate mineral samples is listed in Appendix D. The gas compositions of the samples are given in Table 2 and plotted in Figure 5.

In all of the analyses H₂O is the most abundant gas. The carbon and sulfur gases are the next most abundant and have quantities which are related to sample occurrence. Samples of phyllosilicates from hydrothermally altered rock have several times the carbon and sulfur volatile contents of samples of igneous and metamorphic phyllosilicates. This can

TABLE 2. Petrography and Gas Compositions of Mineral Samples

Sample No.	Rock Type	Alt'n Type	Mineral-ized	Phyllo-silicates	H ₂ O* (mole %)	C	S
Bio 1B	qz-moly vein	pot	yes	bio	82.7	1.2	16.1
SR 1A	qz-cpy vein	pot	yes	bio	98.3	0.3	1.5
SR 1B	qz monz	pot	yes	bio+BIO [±] ser	95.9	3.5	0.6
CSG 1A	gran	-	no	BIO	99.2	0.4	0.3
MD 1A	gran	-	no	BIO [±] MUSC	99.9	0.1	0.1
Bio 2A	peg	-	no	BIO	98.3	1.0	0.8
PM 2A	rhy agгло	prop	yes	chl	98.5	1.4	0.1

TABLE 2. continued

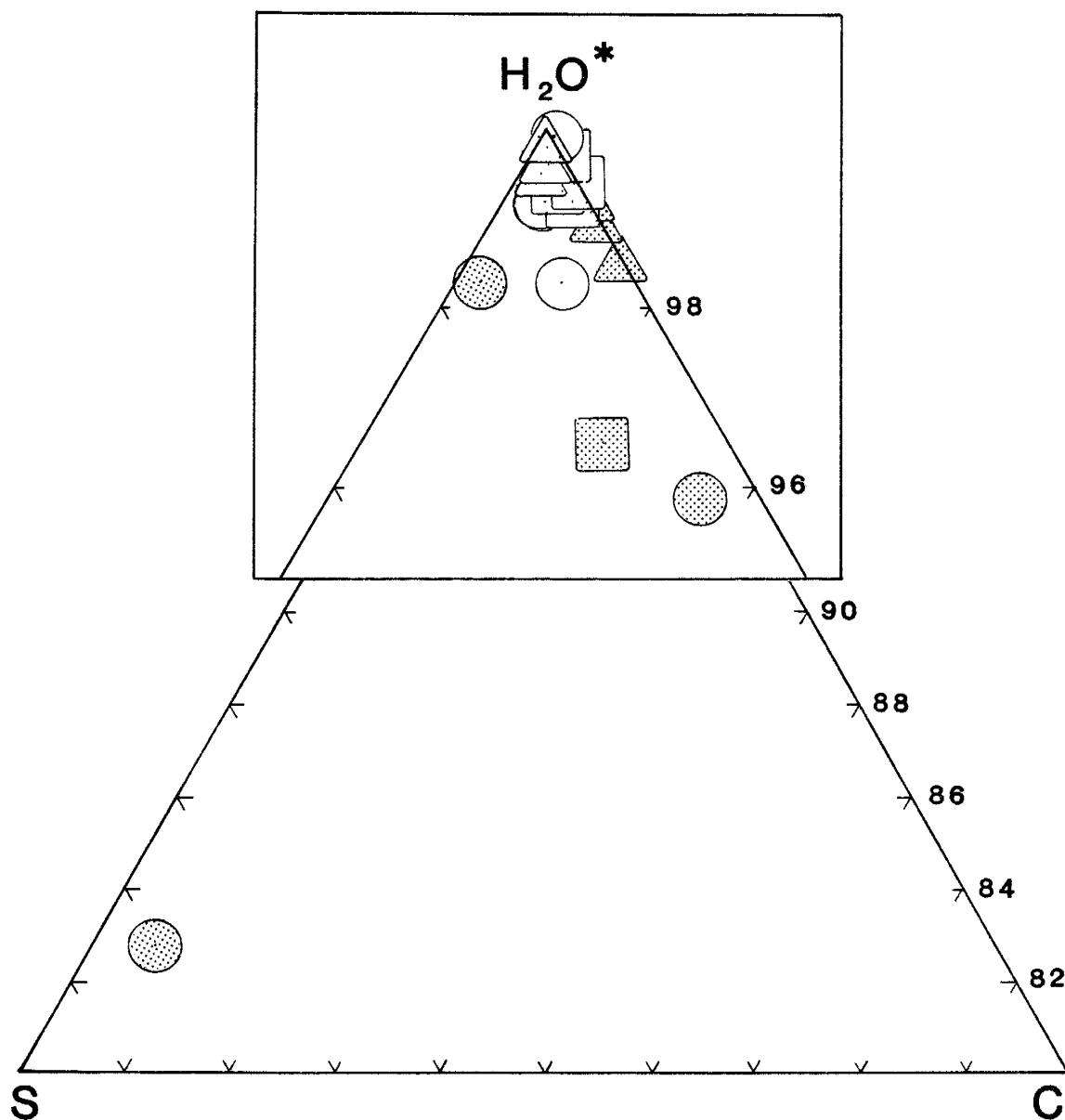
Sample No.	Rock Type	Alt'n Type	Mineral-ized	Phyllo-silicates	H2O*	C (mole %)	S
14TBG 74	qz-cpy	?	yes	chl	99.2	0.8	0.1
Chl 4A	?	prop	yes	chl	99.1	0.9	0.1
Chl 3A	chl schist	-	no	CHL	99.5	0.2	0.3
Chl 2F	kom	-	no	CHL(?)	99.8	0.1	0.1
C 5B	qz lat tuff	ser± adv arg	yes	ser	96.5	2.3	1.2
Mus 2B	peg	-	no	MUSC	99.2	0.7	0.2
Mus 4A	ser schist	-	no	MUSC	99.4	0.6	0.1
Mus 3A	peg	-	no	MUSC	99.7	0.3	0.1

Explanation: adv arg=advanced argillic, agglo=agglomerate, BIO=igneous biotite, bio=hydrothermal biotite, CHL=metamorphic chlorite, chl=hydrothermal chlorite, cpy=chalcopyrite, gran=granite, kom=komatiite, moly=molybdenite, MUSC=igneous or metamorphic muscovite and sericite, peg=pegmatite, pot=potassic, prop=propylitic, qz=quartz, qz lat=quartz latite, qz monz=quartz monzonite, ser=hydrothermal sericite

clearly be seen in Figures 6 and 7 which plot the carbon verses H2O contents and sulfur verses H2O contents of the phyllosilicate mineral samples.

Gas release patterns for biotite, chlorite, and muscovite samples which were step-heated (Fig. 8) indicate the gases are not the product of thermal decipitation of mineral contaminants. The H2O* (defined as H2O + H2) release peaks correspond to temperatures of dehydroxylation of the phyllosilicate structure for these minerals (Hutchinson,

Figure 5. H₂O*-C-S diagram with gas compositions of phyllosilicate mineral samples.



MINERAL

OCCURRENCE

○ Biotite

△ Chlorite

□ Muscovite

▨ Hydrothermal

□ Igneous or Metamorphic

Figure 6. Carbon verses H₂O contents of phyllosilicate mineral samples.

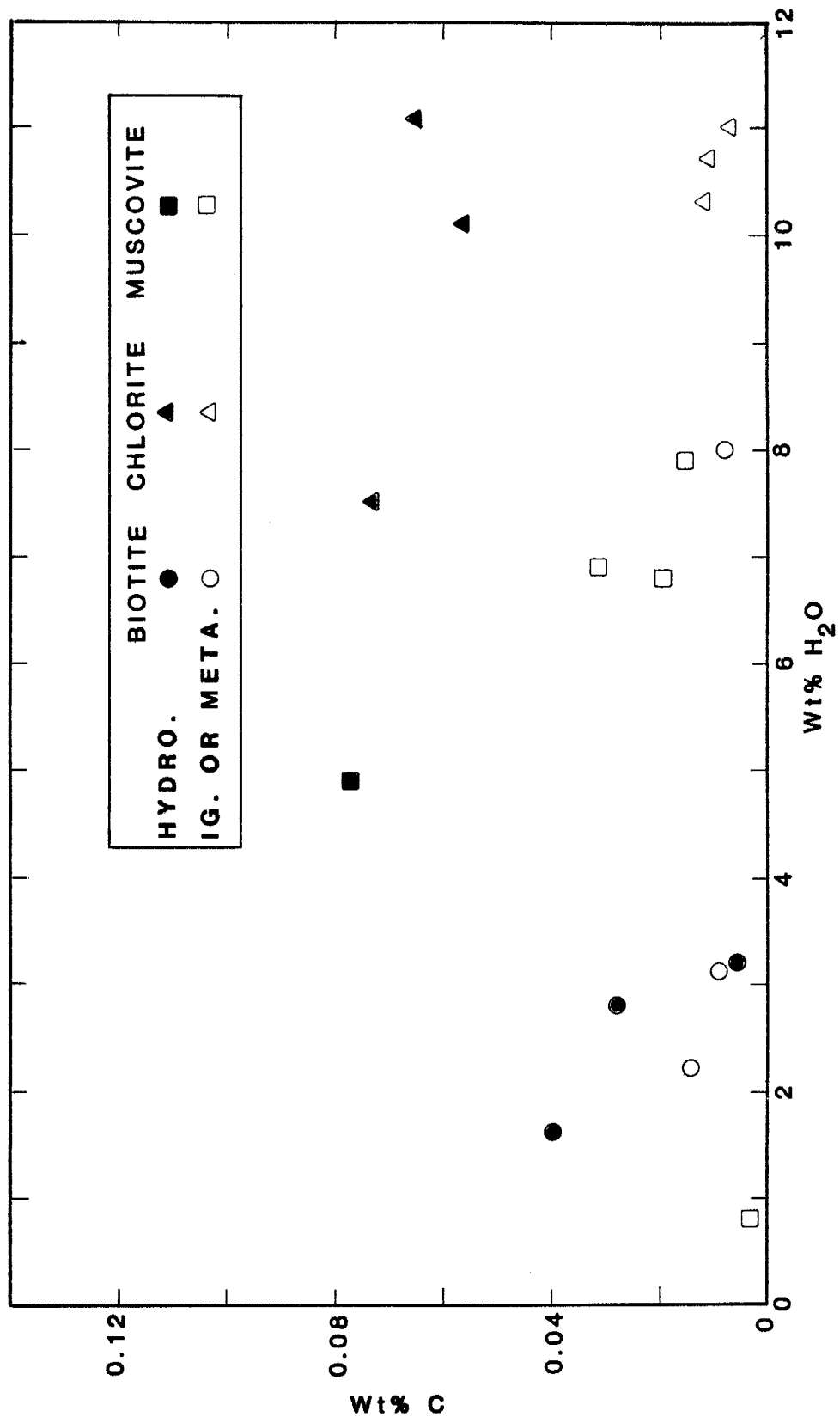


Figure 7. Sulfur verses H₂O contents of phyllosilicate mineral samples.

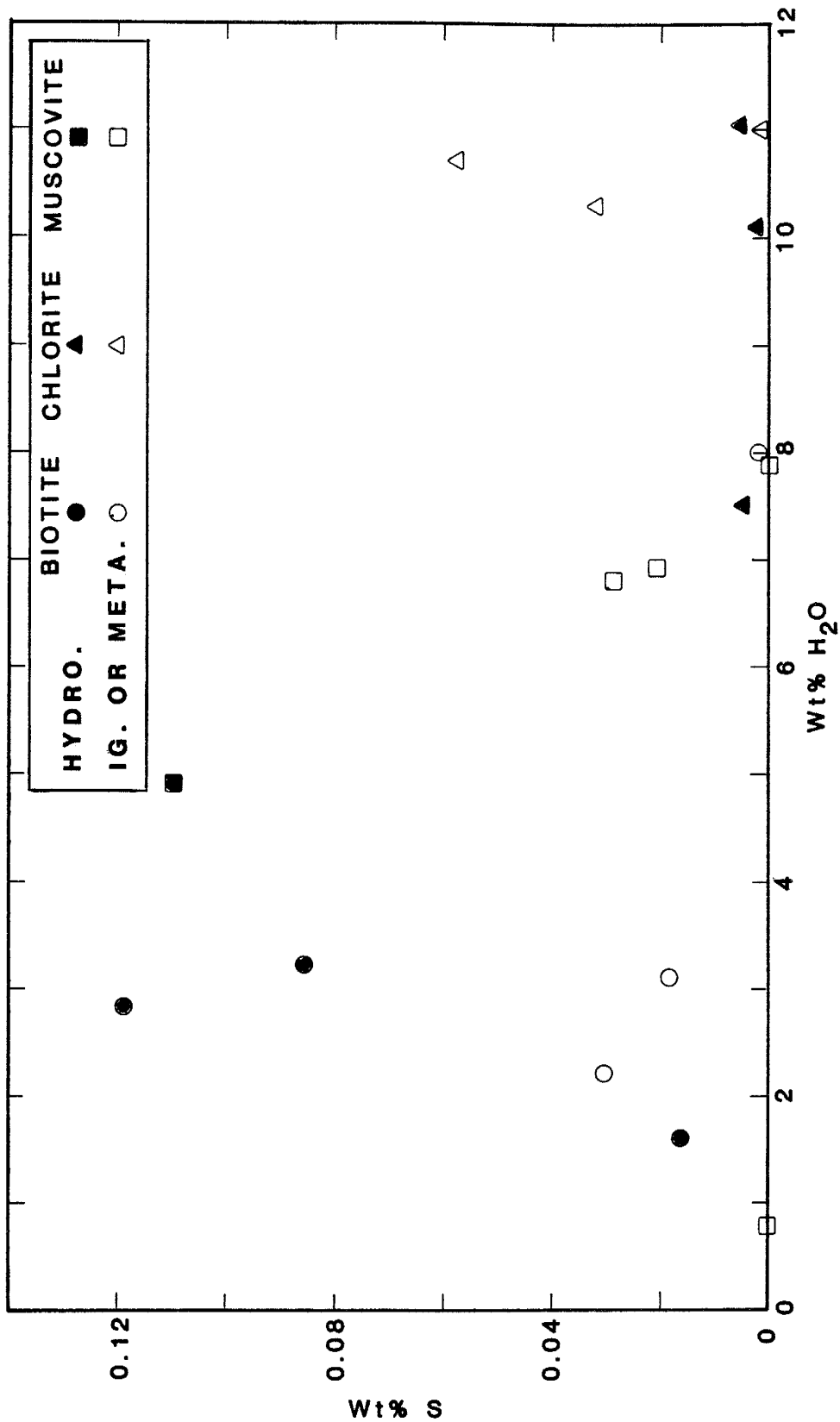
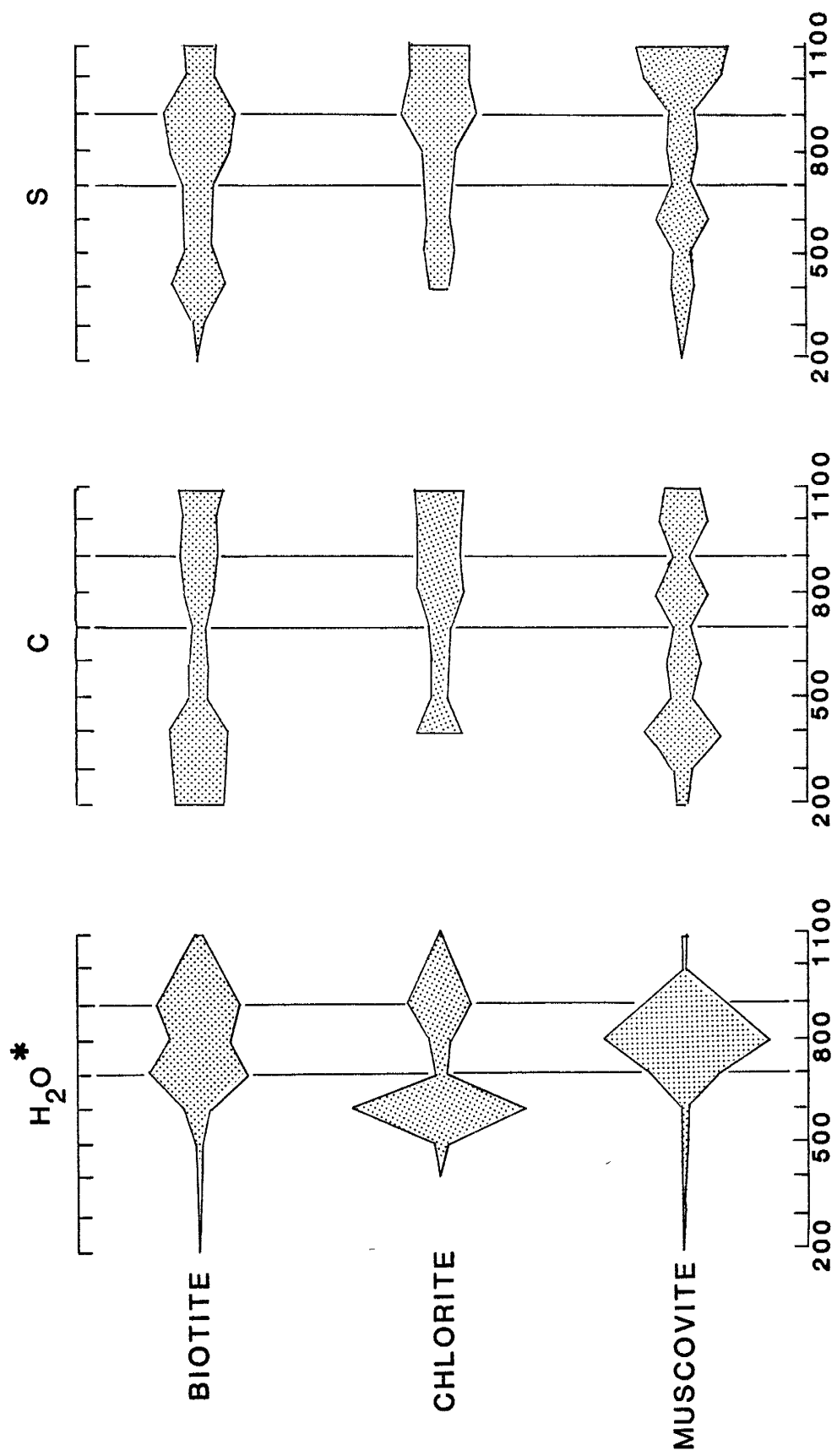


Figure 8. Thermal gas release patterns for samples of biotite (Bio 2A), chlorite (Chl 3A), and muscovite (Mus 2B). The width of the pattern at each temperature is proportional to the fraction of H₂O*, C, or S released at that temperature relative to the total H₂O*, C, or S released from the sample.



Temperature °C

I 10 %

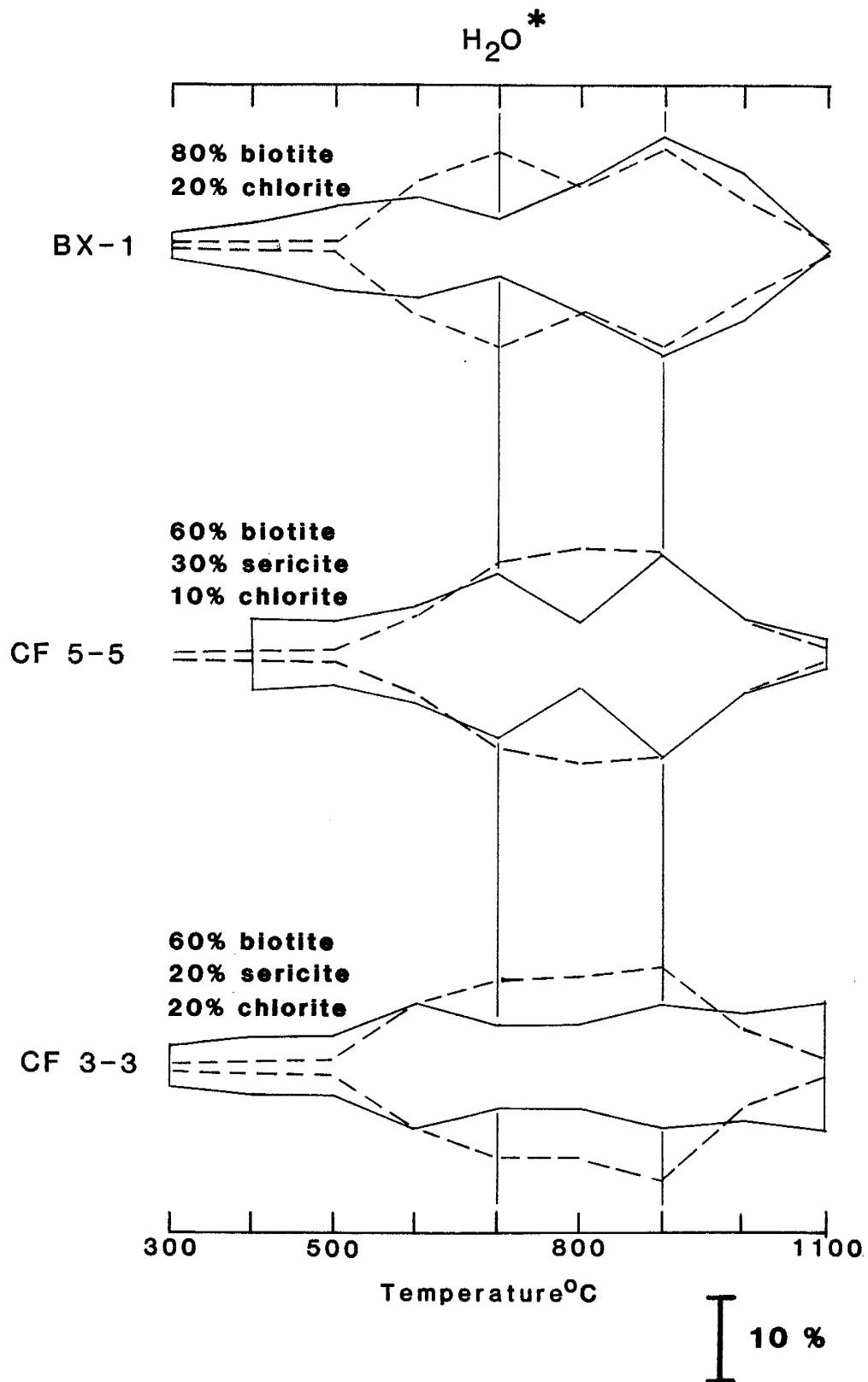
1965; Gerling, et al., 1967; Rimsaite, 1970). Although the source of the carbon and sulfur gases is more difficult to explain and was not within the scope of this study, the release patterns are distinctly different than those produced by thermal breakdown of sulfides and carbonates, which have very narrow temperature ranges (Norman and Palin, 1982) or sulfates, which release O_2 (Ficalora, et al., 1968). This suggests that the carbon and sulfur gases are released from as yet unidentified carbon and sulfur volatiles within the phyllosilicate minerals during thermal decrepitation.

Phyllosilicate-Bearing Rock Samples

Step-heating of three phyllosilicate-bearing rock samples, selected from the suite of samples from the Copper Flat mine, produced the H_2O^* release patterns shown in Figure 9. Also shown in this figure are the H_2O^* release patterns calculated for each sample by linearly combining the mineral release patterns of Figure 8 in a proportion equal to the phyllosilicate mineralogy of the sample.

In general, the observed and calculated patterns do not agree. The observed H_2O^* release peaks are less pronounced than the corresponding calculated H_2O^* release peaks. Two factors contribute to the difference between the observed and calculated H_2O^* release patterns. First, the rock samples were finer grained than the phyllosilicate mineral samples which were step-heated. Since finer grained particles

Figure 9. Observed (solid lines) and calculated (dashed lines) thermal H₂O* release patterns for three phyllosilicate-bearing rock samples. The phyllosilicate mineralogy of each sample is also shown. The method used to calculate H₂O* release patterns is explained in the text. The width of the pattern at each temperature is proportional to the fraction of H₂O* released at that temperature relative to the total H₂O* released from the sample.



undergo more rapid dehydroxylation than coarser grained particles (Delaney, et al., 1978), the observed H₂O* release peaks for the rock samples will occur at temperatures lower than those calculated using the data for the mineral samples. Second, since 100 degree intervals were used in the step-heating analysis, small differences in H₂O* release temperatures will appear much larger if they fall in different heating intervals. Thus, the differences between the observed and calculated H₂O* patterns may be smaller than they appear in Figure 9.

This experiment demonstrates that the gases released from phyllosilicate-bearing rock samples are essentially those of the constituent phyllosilicate minerals. The other minerals of the samples (quartz, plagioclase, and potassium feldspar) release only minor amounts of gas. This is true whether or not the minerals contain a large amount of fluid inclusions. For example, according to Roedder (1979), fluid inclusion-rich minerals usually contain approximately 0.1 vol.% fluid. If the fluid is 100% H₂O and all of the inclusions survive grinding during sample preparation, then a maximum of 0.04 wt.% H₂O can be released from fluid inclusions. The gas data of the present study indicate rock samples release about 1.0 wt.% H₂O. Thus, the maximum contribution to the gas analyses by fluid inclusions is approximately 4%.

Bingham Mine Samples

Sample Descriptions

Ten rock samples were analyzed from the Bingham Mine. They included 3 metasediment samples, 4 monzonite samples, and 1 sample each of quartz monzonite porphyry, porphyritic quartz latite, and latite porphyry collected by staff of the Geology Department of the Utah Copper Division of Kennecott Copper from locations shown in Figure 2d. The following summary descriptions are based on examination of hand specimens and thin sections (see Appendix C for individual sample descriptions).

The metasediment samples are hydrothermally altered, fine-grained, quartzite from the Bingham Mine Formation. They contain 80-90% granular quartz, with variably altered interstitial clay. In propylitically altered samples (B-1 and B-2), clay is partially replaced by chlorite. Sample B-4, which is potassically altered, contains fine-grained hydrothermal biotite replacements of clay. In sample B-2, overprinting by later intermediate argillic alteration has produced sericite replacement of both clay and chlorite.

Monzonite samples are moderate to dark gray, fine-grained, and equigranular. The three samples from the Bingham stock (B-5, B-7, and B-9) are potasically altered, with mafic minerals replaced by fine-grained hydrothermal biotite. The sample from the Last Chance stock (B-6) is

relatively fresh, containing unaltered potassium-feldspar, clinopyroxene, and biotite.

Sample B-3 is from the quartz monzonite porphyry phase of the composite Bingham stock. It is light gray, with medium-grained plagioclase phenocrysts in a fine-grained groundmass of plagioclase, potassium-feldspar, quartz, and biotite. The sample is potassically altered with disseminated, fine-grained, hydrothermal biotite. The feldspars are partially replaced by sericite and calcite, indicating the sample has been overprinted by later intermediate argillic alteration.

The latite samples are from dikes which cross-cut the Bingham stock. Sample B-8 is a relatively fresh latite porphyry with coarse-grained feldspar phenocrysts in a very fine-grained groundmass of feldspar, clinopyroxene, biotite, and quartz(?). Sample B-10 is a intermediate argillically altered porphyritic quartz latite with both medium-grained feldspar phenocrysts and the fine-grained groundmass replaced by very fine-grained sericite.

Gas Analyses

The complete gas analysis of each sample from Bingham is listed in Appendix D. The gas compositions of the samples are given in Table 3 and plotted in Figure 10.

The gas analysis for sample B-1 has 56×10^{-7} moles of H₂O compared to $200-1000 \times 10^{-7}$ moles of H₂O for the other

samples. This difference indicates the H₂O measurement for B-1 may be erroneous and consequently the carbon and sulfur contents appear high. Therefore, sample B-2 is disregarded.

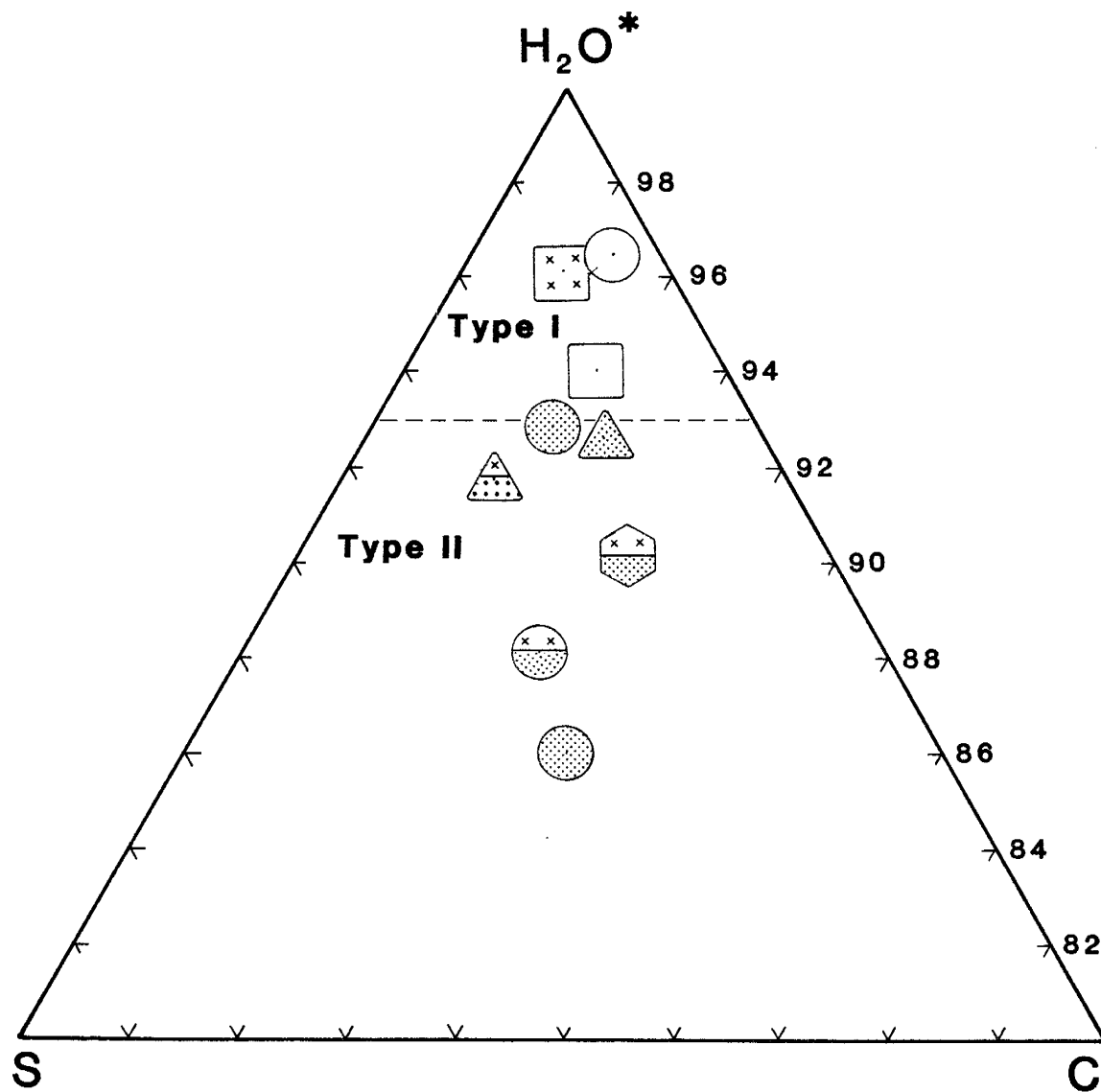
TABLE 3. Petrography and Gas Compositions of Bingham Samples

Sample No.	Rock Type	Alt'n Type	Mineral-ized	Phyllo-silicates	H ₂ O* (mole %)	C	S
B-1	qzite	prop	yes	chl±ser	63.6	15.3	21.1
B-2	qzite	prop+ int arg	yes	chl+ser	91.7	2.7	5.5
B-3	qz monz	pot+ int arg	yes	bio+ser+ BIO	90.0	6.1	3.9
B-4	qzite	pot	yes	bio	92.6	4.4	3.0
B-5	monz	pot	yes	bio+BIO	86.1	7.1	6.9
B-6	monz	-	no	BIO±ser	96.5	2.6	0.9
B-7	monz	pot	yes	BIO+bio	92.9	3.3	3.8
B-8	lat por	-	no	BIO±ser	93.9	3.6	2.5
B-9	monz	pot+ int arg± prop	no	BIO+ser+ bio±chl	88.3	5.4	6.3
B-10	por qz lat	int arg	no	ser+BIO	96.2	1.9	2.0


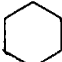


Explanation: BIO=igneous biotite, bio=hydrothermal biotite, chl=hydrothermal chlorite, int arg=intermediate argillic, lat por=latite porphyry, por qz lat=porphyritic quartz latite, pot=potassic, prop=propylitic, qzite=quartzite, qz monz=quartz monzonite, ser=hydrothermal sericite

The samples may be arbitrarily classified according to gas composition (Fig. 10). Type I samples have gas compositions with $(C + S)/(H_2O^* + C + S)$ ratios less than




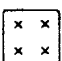
Figure 10. H_2O^* -C-S diagram with gas compositions of Bingham Mine samples. The division between Type I and II samples is at $(\text{C} + \text{S})/(\text{H}_2\text{O}^* + \text{C} + \text{S}) = 0.07$.



ROCK TYPE

-  Latites
-  Qz Monzonite
-  Monzonite
-  Sediments

ALTERATION

-  Fresh
-  Propylitic
-  Potassic
-  Int. Argillic

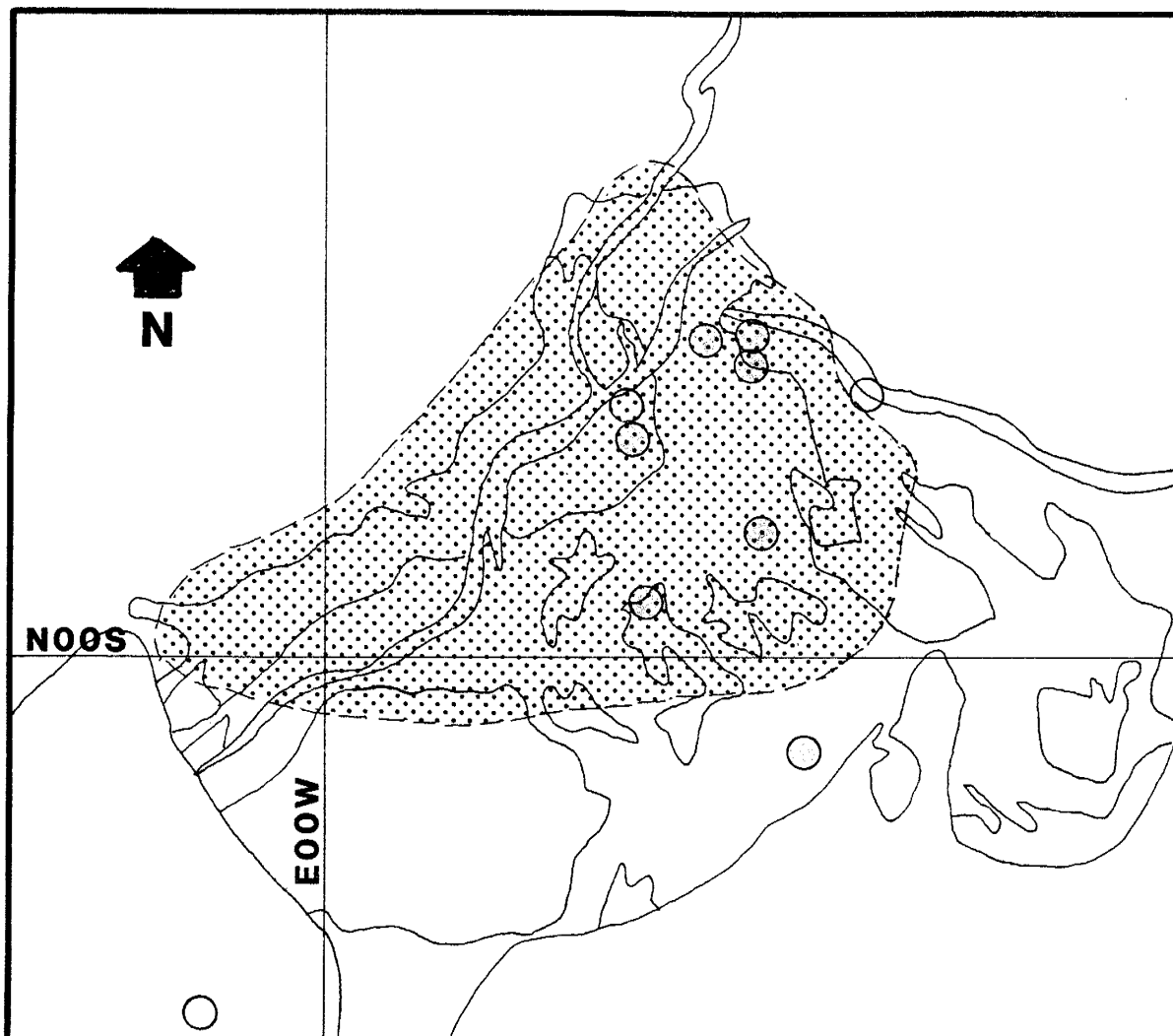
0.07. Type II samples have gas compositions with $(C + S)/(H_2O^* + C + S)$ ratios greater than 0.07.

Type I and Type II samples are compared in Table 4. There are no significant differences in lithology or phyllosilicate mineralogy between Type I or Type II samples. With respect to alteration and mineralization, however, the two sample groups are distinctly different. Type I samples are either relatively unaltered and furthest from the orebody (Fig. 11), or exhibit intermediate argillic alteration and post-date mineralization. Type II samples are potassically or propylitically altered, with some overprint by intermediate argillic alteration. They are within or near to the orebody (Fig. 11).

TABLE 4. Comparison of Type I and Type II Samples from the Bingham Mine

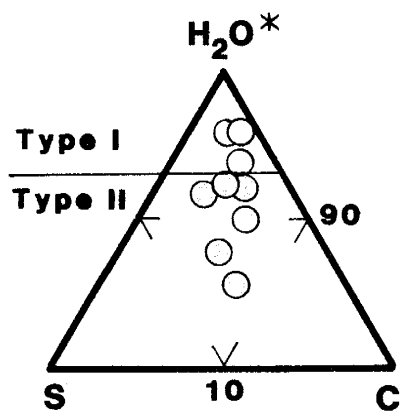
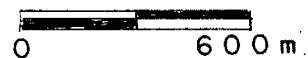
	Type I	Type II
Lithology	monzonite latite porphyry porphyritic quartz latite	monzonite quartz monzonite metasediment
Phyllosilicate Mineralogy	igneous biotite hydrothermal sericite	hydrothermal biotite hydrothermal chlorite igneous biotite hydrothermal sericite
Alteration	fresh intermediate argillic	potassic propylitic intermediate argillic overprints
Mineralization	all samples outside or post-date orebody	5 of 6 samples within orebody

Figure 11. Distribution of Type I and Type II samples at the Bingham Mine. The orebody is shown by the stippled pattern.



EXPLANATION

SCALE



Copper Flat Mine Samples

Sample Descriptions

A suite of rock hand-samples was collected for this study from surface exposures at the Copper Flat Mine. From this suite, 5 samples of andesite, 14 samples of quartz monzonite, and 1 sample of breccia were analyzed. The locations of these samples are given in Figure 4d. The following summary descriptions are based on examination of hand specimens and thin sections (see Appendix C for individual sample descriptions).

Samples CF 2-6, CF 5-1, CF 6-2, CF 7-1, and CF 7-7 are dark greenish gray to brown, fine- to medium-grained, porphyritic, pyroxene andesite. Phenocrysts are mainly medium-grained plagioclase and lesser pyroxene (probably augite) with rims of hornblende. The groundmass is composed of fine- to very fine-grained, interlocking laths of plagioclase and interstitial opaques. All the andesite samples exhibit some degree of propylitic alteration in the form of very fine-grained chlorite, epidote, and calcite in the groundmass. Samples CF 2-6, CF 5-1, and CF 7-7 exhibit intense sericitic alteration overprints.

Samples CF 1-1, CF 1-3, CF 1-5, CF 2-2, CF 2-4, CF 3-1, CF 3-3, CF 3-4, CF 3-5, CF 4-3, CF 5-3b, CF 5-4a, CF 5-5, and CF 6-6 are light tan to gray, coarsely porphyritic to fine-grained equigranular, quartz monzonite of the Copper

Flat stock. The least altered samples contain potassium-feldspar phenocrysts up to 3 cm in length in a fine- to medium-grained groundmass of feldspar, quartz, biotite, and minor hornblende and opaques. Potassically altered samples contain disseminated fine-grained, hydrothermal biotite. Most of the samples exhibit partial replacement of feldspar by sericite and incipient replacement of mafic minerals, including hydrothermal biotite, by sericite and chlorite. These features indicate the samples have been overprinted by sericitic alteration.

Sample BX-1 is from the breccia pipe. It consists of angular, nonrotated clasts of quartz monzonite in a coarse-grained matrix of quartz, biotite, potassium-feldspar, pyrite, chalcopyrite, magnetite, and molybdenite, plus minor fluorite and calcite. Minerals in the matrix range up to 5 cm and occasionally occur with well-terminated crystal faces projecting into open vugs, indicating they grew in open-space.

Gas Analyses

The complete gas analysis of each sample from Copper Flat, including a sample of fluid-inclusion bearing quartz from the matrix of the breccia pipe, is listed in Appendix D. The gas compositions of the samples are given in Table 5 and plotted in Figure 12.

Samples CF 2-6, CF 5-1, and CF 6-2 have gas compositions

with very high levels of carbon and sulfur. In the case of sample CF 6-2, the low amount of H₂O reported suggests the possibility of an erroneous H₂O measurement. Sample CF 2-6 released high amounts of CO₂ and CO, indicating possible contamination by fine-grained calcite, and sample CF 5-1 released high amounts of H₂S and SO₂, indicating possible sulfide contamination. Both these samples exhibit overprints of intense sericitic alteration and contain abundant very fine-grained sericite, calcite, and sulfides which made sample cleaning difficult. Because of these factors, samples CF 2-6, CF 5-1, and CF 6-2 are not included in further discussions of the Copper Flat gas data.

TABLE 5. Petrography and Gas Compositions of Copper Flat Samples

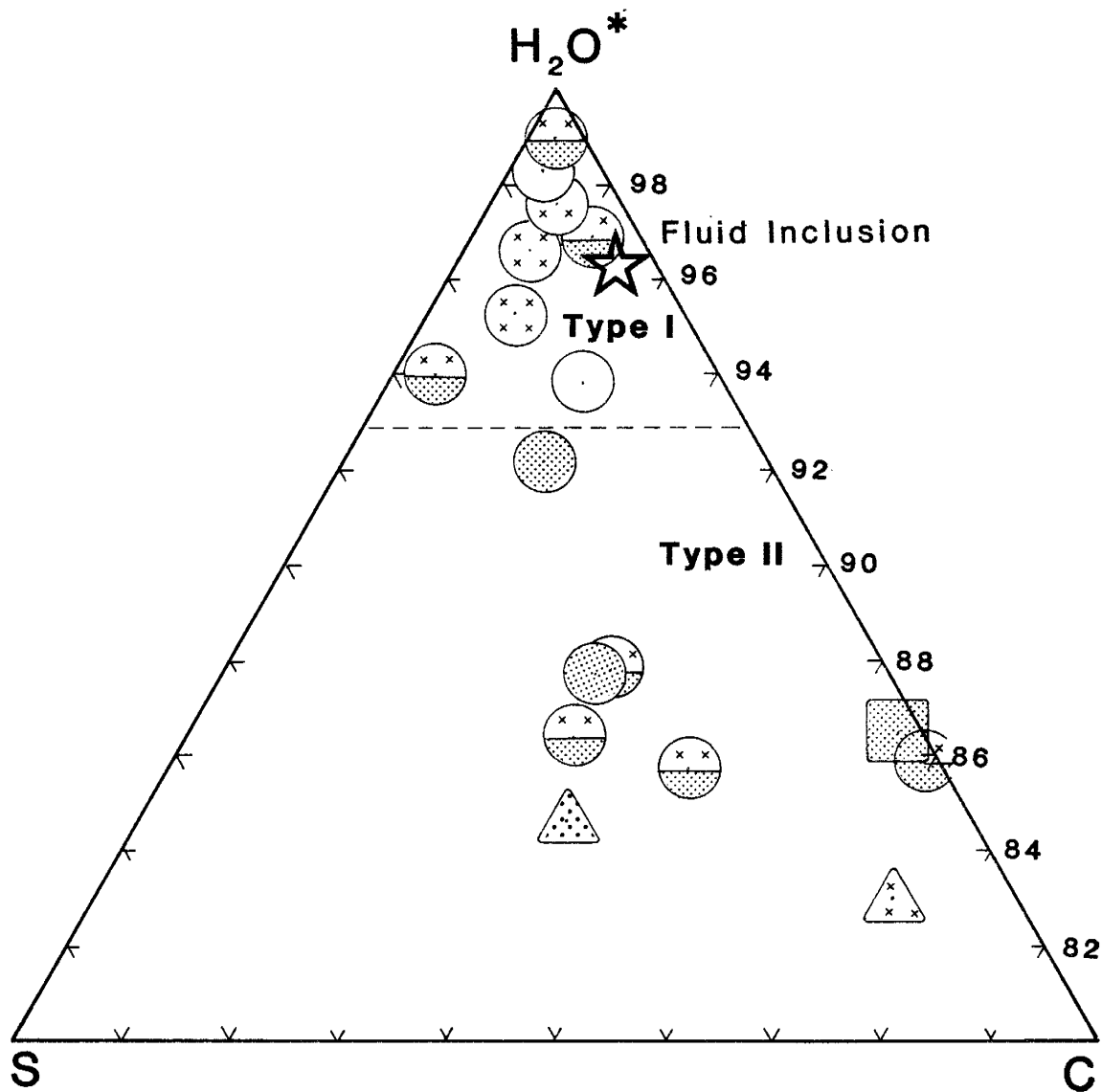
Sample No.	Rock Type	Alt'n Type	Mineral-ized	Phyllo-silicates	H ₂ O* (mole %)	C	S
CF 1-1	qz monz	pot± prop	no	BIO+bio± chl	87.7	6.9	5.4
CF 1-3	qz monz	-	no	BIO	98.3	0.6	1.2
CF 1-5	qz monz	-	no	BIO	93.8	3.6	2.6
CF 2-2	qz monz	pot+ ser	no	ser+BIO+ bio	86.4	7.2	6.5
CF 2-4	qz monz	pot	yes	bio+BIO	92.2	3.8	4.1
CF 2-6	and	ser	no	ser±chl	68.5	31.4	0.1

TABLE 5. Continued

Sample No.	Rock Type	Alt'n Type	Mineral-ized	Phyllo-silicates	H2O* (mole %)	C	S
CF 3-1	qz monz	ser	no	ser	96.7	1.2	2.1
CF 3-3	qz monz	pot+ ser	yes	bio+ser+ BIO	87.8	7.1	5.1
CF 3-4	qz monz	ser	yes	ser±BIO	95.3	1.5	3.1
CF 3-5	qz monz	ser	yes	ser±BIO	97.6	1.1	1.2
CF 4-3	qz monz	pot+ ser	yes	ser+bio± BIO	85.7	9.6	4.7
CF 5-1	and	prop+ ser	no	ser+chl	50.9	10.5	38.5
CF 5-3b	qz monz	pot+ ser	yes	bio+ser+ BIO	94.0	0.8	5.2
CF 5-4a	qz monz	pot+ ser	no	bio+ser+ BIO	99.0	0.5	0.5
CF 5-5	qz monz	pot+ ser	no	bio+ser+ BIO	85.1	14.9	0.1
CF 6-2	and	ser	no	ser	64.0	25.8	10.1
CF 6-6	qz monz	pot+ ser	no	ser+bio+ BIO	96.9	2.2	0.9
CF 7-1	and	prop	no	chl	84.6	7.9	7.5
CF 7-7	and	ser	no	ser	83.0	14.8	2.3
BX-1	bx	pot	yes	bio±chl	86.5	13.1	0.5
fluid incl.	qz	-	-	-	96.3	3.0	0.7

Explanation: and=andesite, BIO=igneous biotite, bio=hydrothermal biotite, bx=breccia, chl=hydrothermal chlorite, pot=potassic, prop=propylitic, qz=quartz, qz monz=quartz monzonite, ser=hydrothermal sericite

Figure 12. H₂O*-C-S diagram with gas compositions of Copper Flat Mine samples. Also shown is the gas composition of a sample of fluid inclusion-bearing quartz (star). The division between Type I and II samples is at $(C + S)/(H_2O^* + C + S) = 0.07$.



ROCK TYPE

□ Breccia

○ Qz Monzonite

△ Andesite

ALTERATION

□ Fresh

▤ Propylitic

▥ Potassic

▧ Sericitic

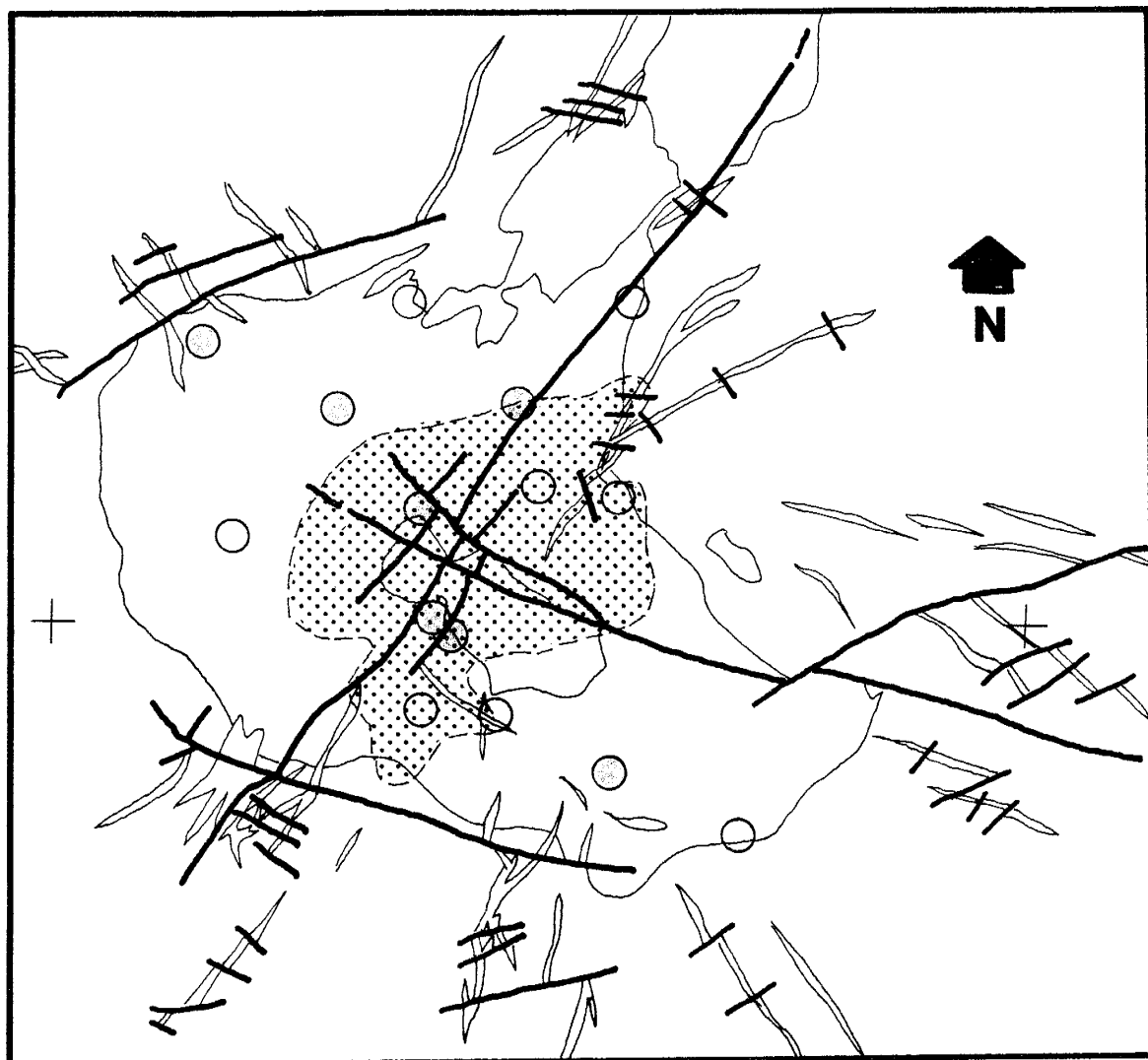
The samples are classified in the same manner as those from Bingham (Fig. 12). Type I samples have $(C + S)/(H_2O^* + C + S)$ ratios less than 0.07. Type II samples have $(C + S)/(H_2O^* + C + S)$ ratios greater than 0.07.

Type I and Type II samples are compared in Table 6. There are no outstanding differences in lithology or phyllosilicate mineralogy between the Type I samples and the Type II samples. There are differences in alteration and mineralization between the sample groups, however. Type I samples are either unaltered or sericitically altered, and are mostly located outside the orebody (Fig. 13). Type II samples are all potassically or propylitically altered, although some have sericitic overprints. Most of the Type II samples are located in the highest grade portions of the orebody (Fig. 13 and Dunn, 1982).

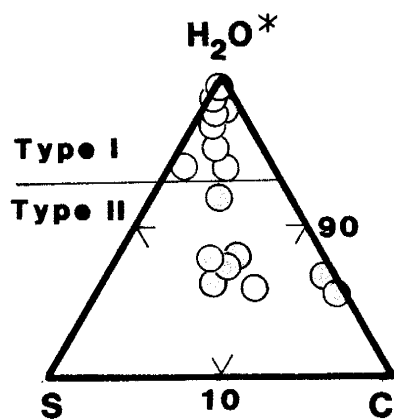
TABLE 6. Comparison of Type I and Type II Samples from the Copper Flat Mine

	Type I	Type II
Lithology	quartz monzonite	quartz monzonite andesite breccia
Phyllosilicate Mineralogy	igneous biotite hydrothermal sericite hydrothermal biotite	hydrothermal biotite igneous biotite hydrothermal sericite hydrothermal chlorite
Alteration	sericitic fresh	potassic propylitic
Mineralization	5 of 8 samples outside orebody	4 of 7 samples within orebody

Figure 13. Distribution of Type I and Type II samples from within the stock at the Copper Flat Mine. The orebody is shown by the stippled pattern.



EXPLANATION



SCALE



DISCUSSION

Interpretation of the Gas Data

The results of this study demonstrate that the composition of gases released from phyllosilicate mineral and phyllosilicate-bearing rock samples is related to their geologic occurrence. Phyllosilicates from hydrothermally altered rocks release more carbon and sulfur gases than do igneous or metamorphic phyllosilicates. Case studies at the Bingham and Copper Flat porphyry copper deposits indicate phyllosilicate-bearing rocks containing main-stage alteration assemblages and copper mineralization release more carbon and sulfur gases than those containing late-stage alteration assemblages. These relationships suggest that phyllosilicates exposed to hydrothermal fluids, and especially those exposed to mineralizing fluids, retain more carbon and sulfur volatiles than phyllosilicates in other geologic environments.

The retention of carbon and sulfur volatiles by phyllosilicates can be represented by an exchange expression,

$$(C + S)_F = (C + S)_M$$

where, $(C + S)_F$ and $(C + S)_M$ are the carbon and sulfur volatile concentrations of the fluid and phyllosilicate mineral respectively. Under equilibrium conditions,

$$K_D = (C + S)_M / (C + S)_F$$

and,

$$\Delta G^{\circ} = - RT \ln K_D$$

$$K_D = \exp (-\Delta G^{\circ} / (RT))$$

where, K_D is the fluid-phylllosilicate distribution coefficient for carbon and sulfur volatiles, ΔG° is the change in free-energy for the exchange, R is the gas constant, and T is the absolute temperature at which the exchange occurs. Thus, the equilibrium concentration of carbon and sulfur volatiles in a phylllosilicate can be considered a function of 1) the carbon and sulfur volatile concentration of the coexisting fluid and 2) the temperature. It is a simplification not to consider each phylllosilicate mineral and carbon and sulfur volatile species individually. However, the paucity of data prevents a more rigorous treatment.

The gas data for phylllosilicate mineral samples implies that 1) hydrothermal fluids have higher carbon and sulfur concentrations than igneous and metamorphic fluids and/or 2) the K_D for carbon and sulfur volatiles is larger for lower temperature, hydrothermal processes than for higher temperature, igneous and metamorphic processes. Similarly, the gas data from the porphyry copper case studies suggests that 1) main-stage hydrothermal fluids have higher carbon and sulfur volatile concentrations than late-stage hydrothermal fluids and/or 2) the K_D for carbon and sulfur volatiles is larger for higher temperature, main-stage processes than for

lower temperature, late-stage processes. Obviously, K_D values cannot be both positively and negatively correlated with temperature. Since volatile species are involved, it seems reasonable to assume that the K_D for carbon and sulfur volatiles is larger at lower temperatures than at higher temperatures. Thus, the higher carbon and sulfur volatile contents of hydrothermal phyllosilicates relative to igneous and metamorphic phyllosilicates can be due to higher carbon and sulfur volatile concentrations in hydrothermal fluids, lower temperatures associated with hydrothermal processes, or a combination of both of these factors. Conversely, the higher carbon and sulfur volatile contents of main-stage alteration assemblages relative to late-stage alteration assemblages in porphyry copper deposits can only be due to higher carbon and sulfur volatile concentrations in main-stage hydrothermal fluids relative to late-stage hydrothermal fluids.

High carbon and sulfur volatile concentrations can be produced in hydrothermal fluids by addition of magmatic carbon and sulfur volatiles (Brimhall and Ghiorso, 1983) or separation of a carbon and sulfur volatile-enriched phase during boiling (Giggenbach, 1977; Ellis, 1979). Fluid boiling is in evidence at both the Bingham and Copper Flat deposits (Moore and Nash, 1974; Dunn and Fowler, 1982) and has been invoked as a mechanism for mineral deposition in hydrothermal systems (Barnes, 1979; Cathes, 1981). This provides a possible genetic link between high levels of

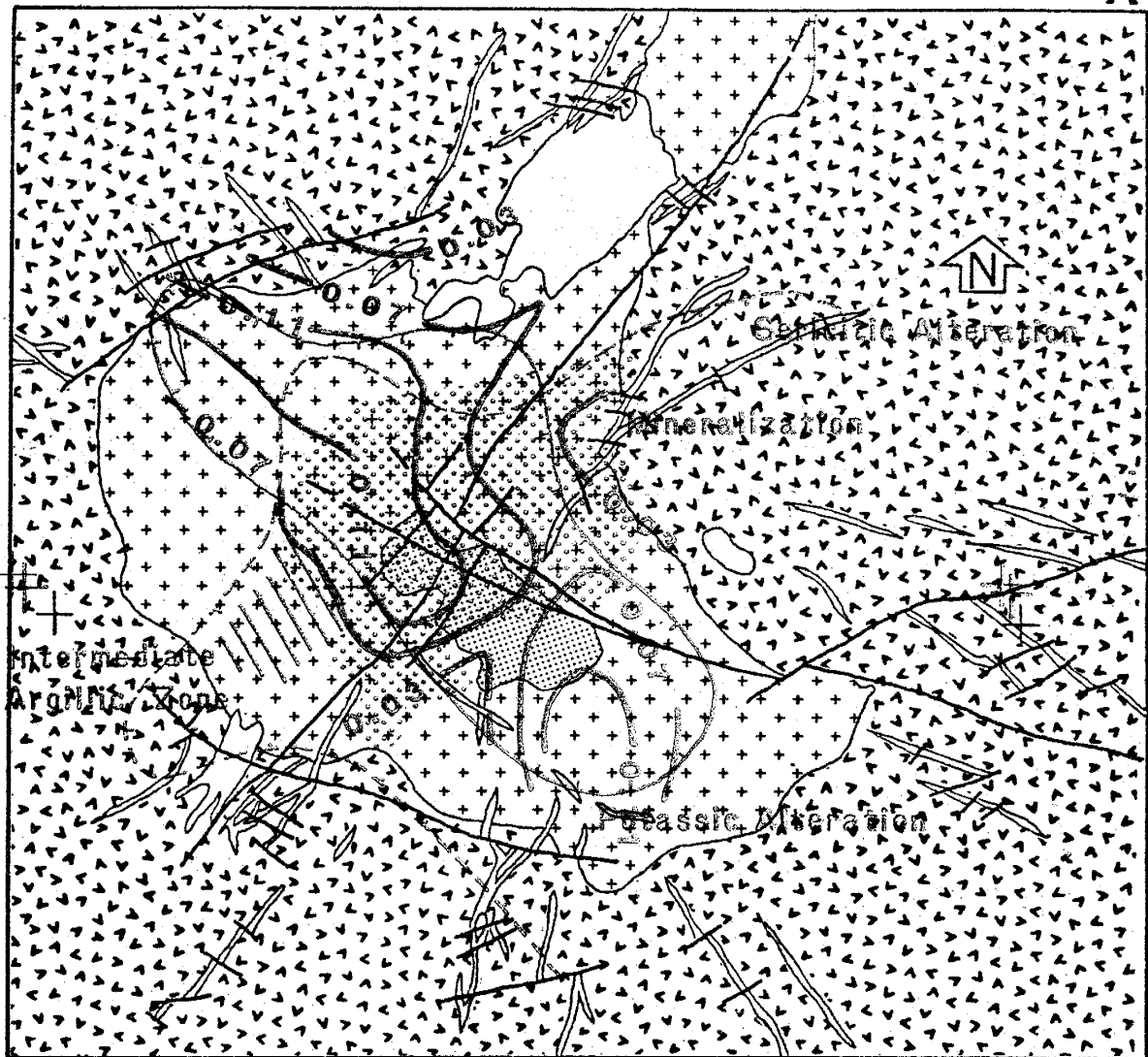
carbon and sulfur volatiles in phyllosilicate minerals and the processes of hydrothermal mineralization.

Application to Mineral Exploration

The case studies at the Bingham and Copper Flat deposits demonstrate that phyllosilicate-bearing alteration assemblages associated with mineralization can be distinguished from those associated with other hydrothermal activity on the basis of the $(C + S)/(H_2O^* + C + S)$ ratios of samples. This suggests that gas analysis of phyllosilicate-bearing rock samples could be used to locate mineralized areas.

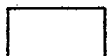
In order to test this hypothesis, the $(C + S)/(H_2O^* + C + S)$ ratios of samples from the Copper Flat Mine were contoured and compared to the surficial geology and distribution of alteration and mineralization at the deposit (Fig. 14). Two features of this plot are significant. First, the largest area of high $(C + S)/(H_2O^* + C + S)$ values lies directly over the western portion of the orebody, which contains the highest copper concentrations. Second, the area of the steepest $(C + S)/(H_2O^* + C + S)$ gradient corresponds to the location of a sharp decrease in the concentration of copper along the southeastern margin of the orebody. Thus, the overall pattern of the $(C + S)/(H_2O^* + C + S)$ ratios reflects the distribution of copper mineralization at Copper Flat and demonstrates the potential of using gas analysis of phyllosilicate-bearing rock as an ore-guide.

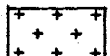
- Figure 14a. Simplified geologic map of the Copper Flat Mine area, New Mexico (from Dunn, 1982).
- b. Distribution of copper mineralization (from Dunn, 1982) and alteration (from this study).
 - c. Contour plot of $(C + S)/(H_2O^* + C + S)$ ratios of samples from the quartz monzonite stock.

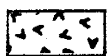


EXPLANATION

 Breccia Pipe

 Latite

 Qz Monzonite

 Andesites

 **Contact**

 **Fault**

SCALE



Suggestions for Further Study

Several aspects of this study deserve further attention. Detailed crystallographic and step-heating studies of phyllosilicates could be done to determine how and in what form carbon and sulfur volatiles are retained in phyllosilicate minerals. Gas analyses of coexisting samples of fluid inclusion-bearing quartz and phyllosilicate minerals from a variety of geologic environments could lead to a better understanding of carbon and sulfur volatile exchange between phyllosilicates and fluids under different physiochemical conditions. A regional study of volcanic samples from around the Copper Flat stock could be done to test the applicability of gas analysis to mineral exploration on a larger scale. In addition, studies of other deposit types, such as epithermal precious metal and volcanic massive sulfide deposits, could be done. Finally, other analytical techniques could be developed to replace mass spectrometry since the results of this study indicate there is no need to identify individual carbon and sulfur gas species in the analysis.

SUMMARY AND CONCLUSIONS

A technique for gas analysis of phyllosilicate-bearing rock has been developed and tested. Analyses of phyllosilicate mineral samples show that water vapor and carbon, sulfur, and nitrogen gases are released upon thermal decrepitation. The amount of carbon and sulfur gases released from phyllosilicates from hydrothermal environments is greater than from phyllosilicates from igneous or metamorphic environments. Release patterns for the carbon and sulfur gases demonstrate that they are not produced from the thermal breakdown of contaminant minerals and suggest they are thermally released from carbon and sulfur volatiles contained in phyllosilicate minerals.

Studies of phyllosilicate-bearing rock samples from the porphyry copper deposits at Bingham, Utah and Copper Flat, New Mexico indicate that gas compositions of samples are related to their alteration and mineralization characteristics. The samples can be divided into two groups based on their gas compositions. Type I samples have $(C + S)/(H_2O^* + C + S)$ ratios less than 0.07 and Type II samples have $(C + S)/(H_2O^* + C + S)$ ratios greater than 0.07. Type II samples are associated with main-stage potassic alteration and copper mineralization, whereas Type I samples are unaltered or associated with late-stage alteration.

The amount of carbon and sulfur volatiles contained in a phyllosilicate minerals can be treated in terms of an

exchange of volatiles between phyllosilicates and coexisting fluids. In this context, the concentration of carbon and sulfur volatiles in phyllosilicates can be considered a function of 1) the carbon and sulfur volatile concentration of the fluids and 2) the temperature at which exchange occurs. The high levels of carbon and sulfur volatiles in phyllosilicates from main-stage alteration assemblages in porphyry copper systems is probably due to exchange with carbon and sulfur volatile-enriched hydrothermal fluids. Such enrichment may be the consequence of processes which also result in mineral deposition.

The results of the case studies at the Bingham and Copper Flat deposits indicate that samples which release gases with the highest $(C + S)/(H_2O^* + C + S)$ ratios are located closest to the respective orebodies. Based on this relationship, gas analysis of phyllosilicate-bearing rock has potential as an ore-guide in hydrothermal mineral deposits.

REFERENCES

- Banks, N. G., 1973, Biotite as a source of some of the sulfur in porphyry copper deposits: *Econ. Geol.*, v. 68, p. 697-702.
- Banks, N. G., 1982, Copper and sulfur in magmas, in: *Advances in Geology of the Porphyry Copper Deposits, Southwestern North America*, S. R. Titley, ed.: Univ. Ariz. Press, Tucson, p. 227-258.
- Barnes, H. L., 1979, Solubilities of ore minerals, in: *Geochemistry of Hydrothermal Ore Deposits*, H. L. Barnes, ed.: John Wiley and Sons, N.Y., p. 404-460.
- Beane, R. E., 1982, Hydrothermal alteration in silicate rocks, in: *Advances in Geology of the Porphyry Copper Deposits, Southwestern North America*, S. R. Titley, ed.: Univ. Ariz. Press, Tucson, p. 117-137.
- Beane, R. E. and Titley, S. R., 1981, Porphyry copper deposits: Part II. Hydrothermal alteration and mineralization: *Econ. Geol. 75th Anniv. Vol.*, p. 235-269.
- Bilodeau, W. L., 1982, Basin configuration as a control on the geometry of Laramide deformation in SE Arizona, SW New Mexico, and NE New Mexico (abstr.): *GSA Abstr. and Prog.*, v. 14, n. 4, p. 147.
- Boyle, R. W., 1979, The geochemistry of gold and its deposits: *Can. Geol. Surv. Bull.* 280, 584p.
- Bray, R. E., 1969, Igneous rocks and hydrothermal alteration at Bingham, Utah: *Econ. Geol.*, v. 64, p. 34-49.
- Brimhall, G. H. and Ghiorso, M. S., 1983, Origin and ore-forming consequences of the advanced argillic alteration process in hypogene environments by magmatic gas contamination of meteoric fluids: *Econ. Geol.*, v. 78, p. 73-90.
- Carapezza, M., Nuccio, P. M., and Valenza, M., 1981, Genesis and evolution of the fumaroles of Vulcano (Aeolian Islands, Italy): a geochemical model: *Bull. Volcano.*, v. 44-3, p. 549-563.
- Cathles, L. M., 1981, Fluid flow and genesis of ore deposits: *Econ. Geol. 75th Anniv. Vol.*, p. 424-457.

- Davis, G. H., 1981, Regional strain analysis of the superposed deformations in southeastern Arizona and the eastern Great Basin, in: Relations of Tectonics to Ore Deposits in the Southern Cordillera: Ariz. Geol. Soc. Digest, v. 14, p. 155-172.
- Delaney, J. R., Muenow, D. W., and Graham, D. G., 1978, Abundance and distribution of water, carbon, and sulfur in the glassy rims of submarine pillow basalts: Geochim. Cosmochim. Acta, v. 42, p. 581-594.
- Dunn, P. G., 1975, Geology of the Copper Flat stockwork breccia, Hillsboro, New Mexico (abstr.): NMGS Annual Field Conf. Guideb., n. 26, p. 337.
- Dunn, P. G., 1981 Geologic studies during the development of the Copper Flat porphyry deposit: Soc. Min. Eng. Preprint 81-3.
- Dunn, P. G., 1982, Geology of the Copper Flat porphyry copper deposit, in: Advances in Geology of the Porphyry Copper Deposits, Southwestern North America, S. R. Titley, ed.: Univ. Ariz. Press, Tucson, p.313-325.
- Dunn, P. G. and Fowler, L. L., 1982, Origin of the Cretaceous Copper Flat porphyry copper deposit, southwestern New Mexico (abstr.): GSA Abstr. and Prog., v. 14, n. 4, p. 161.
- Einaudi, M. T., 1982, Description of skarns associated with porphyry copper plutons, in: Advances in Geology of the Porphyry Copper Deposits, Southwestern North America, S. R. Titley, ed.: Univ. Ariz. Press, Tucson, p.159-163.
- Elinson, M. M., 1970, Research on gas aureoles around Cu-Mo ore bodies (Engl. abstr.): Chem. Abstr., v. 74, n. 5470.
- Ellis, A. J., 1979, Explored geothermal systems, in: Geochemistry of Hydrothermal Ore Deposits, H. L. Barnes, ed.: John Wiley and Sons, N.Y., p. 632-683.
- Evans, B. W., 1969, Chlorine and fluorine in micas of pelitic schists from the sillimanite-orthoclase isograd, Maine: Am. Mineral., v. 54, p. 1209-1211.
- Ficalora, P. J., Uy, O. M., Muenow, D. W., and Margrave, J. L., 1968, Mass spectrometric studies at high temperatures. XXIX. Thermal decomposition and sublimation of alkali metal sulfates: J. Am. Cer. Soc., V. 51, n. 10, p. 574-577.

- Foster, M. D., 1964, Water content of micas and chlorites: USGS Prof. Paper 474-F, p. F1-F15.
- Freund, F., 1980, Carbon in solid solution in forsterite - a key to the untractable nature of reduced carbon in terrestrial and cosmogenic rocks: *Geochim. Cosmochim. Acta*, v. 44. p. 1319-1333.
- Garcia, M. O., Muenow, D. W., and Liu, N. W. K., 1980, Volatiles in Ti-rich amphibole megacrysts, southwest U.S.A.: *Am. Mineral.* v. 65, p. 306-312.
- Garcia, M. D., Liu, N. W. K., and Muenow, D. W., 1979, Volatiles in submarine volcanic rocks from the Marina Island arc and trough: *Geochim. Cosmochim. Acta*, v. 43, p. 305-312.
- Gerling, E. K., 1967, A comparative study of the activation energy of Ar liberation and dehydration energy in amphibole and biotite: *Geochem. Int.*, v. 3, p. 295-306.
- Giggenbach, W. F., 1977, The isotopic composition of sulphur in sedimentary rocks bordering the Taupo volcanic zone, in: *Geochemistry 1977*, A. J. Ellis, ed.: N.Z.D.S.I.R. Bull. 218, p. 57-64.
- Giggenbach, W. F. and LeGuern, F., 1976, The chemistry of magmatic gases from Erta'Ale, Ethiopia: *Geochim. Cosmochim. Acta*, v. 40, p. 25-30.
- Harley, G. T., 1934, The geology and ore deposits of Sierra Co., New Mexico: NM Bur. Mines and Min. Res. Bull, No. 10.
- Hedlund, D. L., 1974, Age and structural setting of base metal mineralization in the Hillsboro - San Lorenzo area, southwestern New Mexico (abstr.): NMGS Annual Field Conf. Guideb., n. 25, p. 378-9.
- Heidrick, T. L. and Titley, S. R., 1982, Fracture and dike patterns in Laramide plutons and their structural and tectonic implications, in: *Advances in Geology of the Porphyry Copper Deposits, Southwestern North America*, S. R. Titley, ed.: Univ. Ariz. Press, Tucson, p. 227-257.
- Henley, R. W. and McNabb, A., 1978, Magmatic vapor plumes and groundwater interaction in porphyry copper emplacement: *Econ. Geol.*, v. 73, p. 1-20.

- Hinkle, M. E. and Kantor, J. A., 1978, Collection and analysis of soil gases emanating from buried sulfide mineralization, Johnson Camp area, Cochise Co., Arizona: *J. Geochem. Explor.*, v. 9, p. 209-216.
- Honma, N. and Itihara, Y., 1981, Distribution of NH_4 in minerals of metamorphic and granitic rocks: *Geochim. Cosmochim. Acta*, v. 45, p. 983-988.
- Hutchison, W. W., 1965, Two stages of decrepitation of micas: *Can. Mineral.*, v. 8, p. 437-460.
- John, E. C., 1978, Mineral zones in the Utah Copper orebody: *Econ. Geol.*, v. 73, p. 1250-1259.
- Killingley, J. S. and Muenow, D. W., 1975, Volatiles from Hawaiian submarine basalts determined by dynamic high temperature mass spectrometry: *Geochim. Cosmochim. Acta*, v. 39, p. 1467-1473.
- Kuellermer, F. J., 1955, Geology of a disseminated Cu deposit near Hillsboro, Sierra Co., New Mexico: *NM Bur. Mines and Min. Res. Circ.* 34.
- Lanier, G., 1978, General geology of the Bingham mine, Bingham Canyon, Utah: *Econ. Geol.*, v. 73, p. 1228-1241.
- LeGuern, F., Gerlach, T. M., and Nohl, A., 1982, Field chromatograph analyses of gases from a glowing dome at Merapi Volcano, Java, Indonesia, 1977, 1978, 1979: *J. of Volc. and Geotherm. Res.*, v. 14, p. 223-245.
- Lovell, J. S., Hale, M., and Webb, J. S., 1980, Vapour geochemistry in mineral exploration: *Min. Mag.*, p. 229-239.
- Lovering, J. F. and Widdowson, J. R., 1968, Electron microprobe determination of sulphur coordination in minerals: *Lithos*, v. 1, p. 264-267.
- Mercer, P. D., 1967, Analysis of the gases released on cleaving muscovite mica in ultrahigh vacuum and of gases which remain absorbed on the freshly cleaved surface: *Vacuum*, v. 17, n. 5, p. 267-70.
- Moore, W. J., 1978, Chemical characteristics of hydrothermal alteration at Bingham, Utah: *Econ. Geol.*, v. 73, p. 1260-1269.

- Moore, W. J. and Czamanske, G. K., 1973, Compositions of biotites from unaltered and altered monzonite rocks in the Bingham mining district, Utah: *Econ. Geol.*, v. 68, p. 269-274.
- Moore, W. J. and Nash, J. T., 1974, Alteration and fluid inclusion studies of the porphyry copper orebody at Bingham, Utah: *Econ. Geol.*, v. 69, p. 631-645.
- Muenow, D. W., Graham, D. G., Liu, N. W. K., and Delaney, J. R., 1979, The abundance of volatiles in Hawaiian tholeiitic submarine basalts: *Earth and Planetary Sci. Let.*, v. 42. p. 71-76.
- Muenow, D. W., Liu, N. W. K., Garcia, M. O., and Saunders, A. D., 1980, Volatiles in submarine volcanic rocks from the spreading axis of the East Scotia Sea back-arc basin: *Earth and Planetary Sci. Let.*, v. 47, p. 3272-278.
- Munoz, J. L. and Ludington, S. D., 1974, Fluorine-hydroxyl exchange in biotite: *Am. J. Sci.*, v. 274, p. 396-413.
- Mysen, B. O., Eggler, D. H., Seitz, M. G., and Holloway, J. R., 1976, Carbon dioxide in silicate melts and crystals. Part I. Solubility measurements: *Am. J. Sci.*, v. 276, p. 455-79.
- Nash, W. P., 1976, Fluorine, chlorine, and OH-bearing minerals in the Skaergaard Intrusion: *Am. J. Sci.*, v. 376, p. 546-556.
- Norman, D. I., 1977, Geology and geochemistry of the Tribag deposit, Balchawana Bay, Ontario: Unpubl. Ph.D thesis, Univ. Minnesota.
- Norman, D. I., 1983, Gases in epithermal Ag-Au fluids (abstr.): *GSA Abstr. and Prog.*, v. 15, n.6, p. 654.
- Norman, D. I. and Palin, J. M., 1982, Volatiles in phyllosilicate minerals: *Nature*, v. 296, p. 551-553.
- Norton, D. L., 1982, Fluid and heat transport phenomena typical of copper-bearing pluton environments, in: *Advances in Geology of the Porphyry Copper Deposits, Southwestern North America*, S. R. Titley, ed.: Univ. Ariz. Press, Tucson, p. 59-72.
- Piperov, N. B. and Penchev, N. P., 1973, A study on gas inclusions in minerals, analysis of micro-inclusions in allanite: *Geochim. Cosmochim. Acta*, v. 37, p. 2075-2097.

- Reeves, C. C., Jr., 1963, Economic geology of a part of the Hillsboro, New Mexico, Mining district: Econ. Geol., v. 58, p. 1278-84.
- Rimsaite, J., 1970, Structural formulae of oxidized and hydroxyl-deficient micas and decomposition of hydroxyl group: Contrib. Min. Petr., v. 25, p. 225-240.
- Roedder, E., 1979, Fluid inclusions as samples of ore fluids, in: Geochemistry of Hydrothermal Ore Deposits, H. L. Barnes, ed.: John Wiley and Sons, N.Y., p.684-737.
- Segerstrom K. and Antweiler, J. C., III, 1975, Placer-gold deposits of the Las Animas district, Sierra County, New Mexico: USGS open-file report.
- Schuiling, R. D. and Kreulen, R., 1979, Are thermal domes heated by CO₂-rich fluids from the mantle?: Earth and Planet. Sci. Let., v. 43, p. 298-302.
- Shephard, E. S., 1938, The gases in rocks and some related problems: Am. J. Sci., v. 35A, p. 311-51.
- Sillitoe, R. H., 1973, The tops and bottoms of porphyry copper deposits: Econ. Geol., v. 68, p. 799-815.
- Smith, W. H., 1978, Geologic map of the Bingham mine: Unpubl. map, Kennecott Copper Corporation, Utah Copper Division.
- Stacey, J. S. and Hedlund, D. C., 1983, Lead-isotopic compositions of diverse igneous rocks and ore deposits from southwestern New Mexico and their implications for early Proterozoic crustal evolution in the western U.S.: GSA Bull., v. 94, p. 43-57.
- Stringham, B., 1953, Granitization and hydrothermal alteration at Bingham, Utah: GSA Bull., v. 64, p. 945-992.
- Taylor, C. H., Kesler, S. E., and Cloke, P. L., 1982, Sulfur gases produced by the decomposition of sulfide minerals: Application to geochemical exploration: J. Geochem. Explor., v. 17, p. 165-185.
- Titley, S. R., 1982, The style and progress of mineralization and alteration in porphyry copper systems, in: Advances in Geology of the Porphyry Copper Deposits, Southwestern North America, S. R. Titley, ed.: Univer. Ariz. Press, Tucson, p. 93-116.

Vedder, W., 1965, Ammonium in muscovite: *Geochim. Cosmochim. Acta*, v. 29, p. 221-228.

Warnaars, F. W., Smith, W. H., Bray, R. E., Lanier, G., and Shafigullah, M., 1978, Geochronology of igneous intrusions and porphyry copper mineralization at Bingham, Utah: *Econ. Geol.*, v. 73, p. 1242-1249.

APPENDIX A

Definitions and Terminology

Igneous Rock Classification:

IUGS Subcommittee on the Systematics of Igneous Rocks,
1973, in: *Geotimes*, v. 18, n. 10, p. 26-30.

Alteration Classification:

Rose, A. W. and Burt, D. M., 1979, Hydrothermal
alteration, in: *Geochemistry of Hydrothermal Ore
Deposits*, H. L. Barnes, ed.: John Wiley and Sons, N.Y., p.
173-235.

Mineralogic Classification:

Hand Samples- Hurlbut, C. S. and Klein, C., 1977, *Manual
of Mineralogy*: John Wiley and Sons, N.Y.

Thin Sections- Kerr, P. F., 1977, *Optical Mineralogy*:
McGraw-Hill, N.Y.

APPENDIX B
Analytical Errors

	Sensitivity	Error
Pressure Measurement (1)	± 0.002 torr	2%
Volume Calibration (2)	± 2 ml	0.5%
Composition Calculation (3)		10%
Weight of H ₂ O (1)	± 0.2 mg	10%
Moles of Individual Gas Species (4)		12%
Moles of H ₂ O (1)		10%
H ₂ O*-C-S Compositions (4)	± 0.3 mole%	

-
- (1) Based on instrument sensitivity.
 - (2) Measured.
 - (3) Estimated.
 - (4) Calculated using typical values.

APPENDIX C

Sample Descriptions

Phyllosilicate Mineral Samples

PM-2A

Fine-grained chlorite in altered rhyolite agglomerate from the Pecos massive sulfide deposit, New Mexico.

14-TBG-74

Medium- to fine-grained chlorite with quartz and chalcopryrite in breccia pipe matrix from the Tribag copper deposit, Ontario, Canada.

Chl 4A

Fine-grained chlorite in alteration pipe from the Buchans massive sulfide deposit, Newfoundland, Canada.

Chl 3A

Fine-grained chlorite schist from northern New Mexico.

Chl 2F

Coarse-grained chlorite in altered komatiite from New Mexico.

C 5B

Massive, fine-grained, sericite-clay altered quartz latite lithic tuff from Amythest-OH vein system (epithermal silver deposit), Creede, Colorado.

Mus 2B

Very coarse-grained muscovite in Bjertnes pegmatite, Norway.

Mus 4A

Fine-grained sericite schist from northern New Mexico.

Mus 3A

Coarse-grained muscovite in pegmatite, New Hampshire.

Bio 1B

Medium-grained biotite in quartz-molybdenite veins from the Questa porphyry molybdenum deposit, New Mexico.

SR 1A

Medium-grained biotite in quartz-chalcopyrite veins from the Santa Rita porphyry copper deposit, New Mexico.

SR 1B

Fine-grained, secondary biotite disseminated in altered quartz monzonite from the Santa Rita porphyry copper deposit, New Mexico.

CSG 1A

Medium-grained biotite in the Cold Springs granite, Minnesota.

MD 1A

Medium-grained biotite in the Mayo-Darle tin-granite, Cameroon.

Bio 2A

Very coarse-grained biotite in pegmatite, northern New Mexico.

Bingham Mine Samples

B-1

Moderate propylitically altered, fine-grained quartzite from the Bingham Mine Formation. Intergranular clays replaced by chlorite. Slightly oxidized disseminated fine-grained pyrite and chalcopyrite.

B-2

Propylitically altered, fine-grained quartzite from the Bingham Mine Formation showing overprinting of intermediate argillic alteration. Intergranular clays replaced by chlorite and calcite which are replaced by sericite. Minor, disseminated, fine-grained pyrite and chalcopyrite.

B-3

Potassically altered, fine-grained quartz monzonite porphyry from the Bingham stock with variable overprinting of intermediate argillic alteration. Disseminated, fine-grained, secondary biotite. Plagioclase phenocrysts and groundmass potassium-feldspar replaced by sericite and minor calcite. Disseminated, fine-grained pyrite and chalcopyrite.

B-4

Potassically altered, fine-grained quartzite from the Bingham Mine Formation. Disseminated, very fine-grained, secondary biotite and fine-grained pyrite.

B-5

Intense potassically altered, fine-grained monzonite from the Bingham stock. Abundant, disseminated, fine-grained, secondary biotite (some aggregates replacing mafic minerals?). Very fine-grained pyrite and chalcopyrite associated with biotite.

B-6

Relatively fresh, fine-grained monzonite from the Last Chance stock. Unaltered potassium-feldspar, clinopyroxene, and lesser biotite with slight replacement of plagioclase by sericite. Fine-grained pyrite associated with mafic minerals.

B-7

Potassically altered, fine-grained monzonite from the Bingham stock. Both original and disseminated, secondary, fine- to very fine-grained biotite. Fine-grained pyrite and chalcopyrite associated with biotite. Some introduced silica in the form of coarse-grained quartz.

B-8

Relatively fresh, fine-grained latite porphyry from small intrusive body in the Bingham stock. Unaltered, very fine- to fine-grained clinopyroxene and fine-grained biotite with slight replacement of coarse-grained feldspar phenocrysts by sericite. Minor, disseminated, very fine-grained pyrite.

B-9

Potassically altered, fine-grained monzonite from the Bingham stock with some overprinting of propylitic (?) alteration. Disseminated, very fine- to fine-grained biotite replaced by chlorite in places. Some medium- to fine-grained feldspar completely replaced by sericite.

B-10

Intense to moderate intermediate argillically altered, porphyritic quartz latite from a large dike cutting the Bingham Mine Formation. Very fine-grained aggregates of sericite replacing all feldspar phenocrysts. Fine-grained pyrite as disseminations and in veinlets.

Copper Flat Mine Samples

CF 1-1

Potassically altered, medium-grained, equigranular quartz monzonite. Disseminated, fine- to medium-grained, secondary biotite showing minor replacement by chlorite. Disseminated, fine-grained pyrite.

CF 1-3

Relatively fresh, quartz monzonite porphyry. Coarse-grained feldspar phenocrysts in a sutured, fine- to medium-grained groundmass.

CF 1-5

Relatively fresh, fine- to medium-grained equigranular quartz monzonite. Biotite showing minor replacement by chlorite.

CF 2-2

Intense sericitically altered, medium-grained, equigranular quartz monzonite. All feldspars and mafics replaced by sericite.

CF 2-4

Potassically altered, porphyritic quartz monzonite. Coarse-grained feldspar phenocrysts in a medium-grained, equigranular groundmass. Disseminated, fine-grained, secondary biotite and pyrite.

CF 2-6

Very intense sericitically altered andesite. Rock replaced by very fine-grained quartz and sericite with abundant, brown iron oxide staining.

CF 3-1

Weak sericitically altered, quartz monzonite porphyry. Medium-grained feldspar and mafic phenocrysts in a fine-grained, sutured groundmass. Minor sericite replacement of feldspar. Minor, brown iron oxide staining.

CF 3-3

Sericitically altered, medium-grained, equigranular quartz monzonite. Feldspars and some biotite replaced by sericite. Disseminated, fine-grained pyrite and chalcopyrite.

CF 3-4

Intense sericitically altered, medium-grained, equigranular quartz monzonite. Feldspars and some biotite replaced by sericite. Disseminated, fine-grained pyrite and chalopyrite.

CF 3-5

Intense sericitically altered, medium-grained, equigranular quartz monzonite. Feldspars and mafics replaced by sericite with brown iron oxide staining.

CF 4-3

Intense sericitically altered, medium-grained, equigranular quartz monzonite. Feldspar replaced by sericite with brown iron oxide staining. Disseminated, fine-grained pyrite and chalcopyrite.

CF 5-1

Sericitically altered, medium-grained, pyroxene andesite. Clinopyroxene with hornblende rims partially replaced by fine-grained chlorite. Feldspar replaced by sericite. Abundant, disseminated, fine-grained pyrite.

CF 5-3b

Potassically altered, quartz monzonite porphyry with overprint of sericitic alteration. Medium- to coarse-grained feldspar phenocrysts in a fine-grained, sutured groundmass. Disseminated, fine-grained, secondary biotite. Feldspar replaced by sericite. Abundant, disseminated, fine-grained pyrite and chalcopyrite with thin quartz veinlets.

CF 5-4a

Potassically altered, quartz monzonite porphyry with overprint of sericitic alteration. Coarse-grained feldspar phenocrysts in a fine- to medium-grained equigranular groundmass. Disseminated, fine-grained, secondary biotite. Feldspar replaced by sericite. Disseminated, fine-grained pyrite and chalcopyrite. Thin quartz ± chalcopyrite ± pyrite veinlets.

CF 5-5

Potassically altered, medium-grained, equigranular quartz monzonite with overprint of intense sericitic alteration. Disseminated, fine-grained, secondary biotite. Feldspar and some biotite replaced by sericite. Disseminated, fine-grained pyrite and thin quartz ± pyrite veinlets.

CF 6-2

Weak sericitically altered, fine-grained pyroxene andesite. Clinopyroxene with hornblende rims. Zoned plagioclase with cores replaced by sericite. Abundant, disseminated, fine-grained pyrite.

CF 6-6

Potassically altered, quartz monzonite porphyry with overprint of intense sericitic alteration. Disseminated, fine-grained, secondary biotite. Feldspar and some biotite replaced by sericite. Abundant, disseminated, fine-grained pyrite.

CF 7-1

Relatively fresh, porphyritic andesite. Medium-grained clinopyroxene phenocrysts in a fine-grained groundmass. Disseminated, fine-grained pyrite.

CF 7-7

Intense sericitically altered, porphyritic andesite. Fine-grained clinopyroxene and feldspar phenocrysts in a very fine-grained groundmass. Abundant, sericite replacement of groundmass and feldspar phenocrysts. Abundant, disseminated, fine-grained pyrite.

APPENDIX D

Gas Analyses of Phyllosilicate Mineral Samples

Sample	BiolB	SR1A	SR1B	CSG1A	MD1A	Bio2A*	PM2A	14TBG	Chl14A
Mineral	bio	bio	bio	BIO	BIO	BIO	chl	chl	chl
Gas (X 10 ⁻⁷ moles)									
H2O	730	1300	940	2900	6000	340	2800	6200	7300
H2	27	140	25	300	37	280	-	-	12
CO2	1.9	3.4	18	9.0	3.4	3.2	34	45	40
CO	8.6	0.4	8.3	0.3	-	2.5	5.8	5.5	6.3
CH4	0.8	0.1	9.2	5.2	3.8	0.3	1.4	1.0	17
C2H6	-	-	2.9	1.5	1.2	-	-	-	-
H2S	140	22	5.0	9.4	0.7	4.6	0.3	1.0	1.8
SO2	3.8	0.8	0.7	1.7	0.1	0.2	0.7	-	0.5
N2	0.5	-	1.0	0.9	1.1	-	1.5	-	1.5
NH3	6.5	0.5	-	0.7	-	0.4	-	-	-

Sample	Chl3A	Chl3A*	Chl2F	C5B	Mus2B	Mus2B*	Mus4A	Mus3A
Mineral	CHL	CHL	CHL	ser	MUSC	MUSC	MUSC	MUSC
Gas (X 10 ⁻⁷ moles)								
H2O	3600	4300	7200	1900	1100	2200	1700	6600
H2	13	99	7.6	36	0.8	24	18	15
CO2	5.2	7.3	5.9	14	3.5	3.3	8.0	3.7
CO	0.4	0.4	0.6	28	2.0	2.7	0.8	10
CH4	0.1	0.2	4.3	3.8	2.0	3.4	1.9	2.6
C2H6	-	-	-	-	-	7.4	3.4	1.5
H2S	8.7	7.0	0.3	23.4	1.1	4.1	0.3	-
SO2	2.3	0.9	0.1	1.5	0.8	1.2	-	-
N2	-	-	0.4	-	-	-	-	-
NH3	1.0	2.3	-	-	-	-	-	-

Gas Analyses of Bingham Mine Samples

Sample	B-1	B-2	B-3	B-4	B-5
Rock Type	qzite	qzite	qz monz	qzite	monz
Gas (X 10 ⁻⁷ moles)					
H2O	56	560	220	170	330
H2	5.6	20	9.2	26	24
CO2	2.5	4.0	2.1	2.7	2.8
CO	12	13	8.8	13	6.6
CH4	0.34	0.31	0.13	0.37	0.29
C2H6	1.4	1.8	1.9	3.5	1.4
H2S	17	23	7.0	5.9	1.4
SO2	3.4	12	0.43	9.7	1.8
N2	5.4	2.4	2.8	5.0	2.8
NH3	-	-	-	-	-

Sample	B-6	B-7	B-8	B-9	B-10
Rock Type	monz	monz	lat por	monz	qz lat
Gas (X 10 ⁻⁷ moles)					
H2O	780	220	330	280	1200
H2	24	27	27	17	9.7
CO2	3.5	6.1	4.7	2.4	1.1
CO	25	8.5	19	8.5	22
CH4	0.34	0.51	0.48	0.51	0.33
C2H6	2.5	1.5	6.1	2.2	1.0
H2S	23	3.7	13	3.8	3.9
SO2	10	14	2.4	4.0	21
N2	2.0	3.8	10	4.9	4.8
NH3	-	-	-	-	-

Gas Analyses of Copper Flat Mine Samples

Sample	1-1	1-3	1-5	2-2	2-4	2-6	3-1
Rock Type	qzmonz	qzmonz	qzmonz	qzmonz	qzmonz	and	qzmonz
Gas (X 10 ⁻⁷ moles)							
H2O	170	4400	610	610	1700	220	2000
H2	9.4	2.4	11	4.0	1.8	0.7	4.3
CO2	3.7	17	6.2	11	37	61	13
CO	10	8.7	17	39	32	40	11
CH4	0.26	-	1.2	0.62	1.2	1.1	0.70
C2H6	0.97	2.1	2.5	1.7	4.9	-	1.6
H2S	-	5.6	2.4	-	7.1	-	3.4
SO2	11	46	15	46	66	0.29	40
N2	5.7	4.9	11	13	4.1	-	5.4
NH3	-	-	-	-	-	-	-

Sample	3-3	3-4	3-5	4-3	5-1	5-3	5-4
Rock Type	qzmonz	qzmonz	qzmonz	qzmonz	and	qzmonz	qzmonz
Gas (X 10 ⁻⁷ moles)							
H2O	220	1100	3900	610	170	2800	4400
H2	3.5	1.0	4.9	14	19	5.8	13
CO2	6.4	9.9	22	40	31	8.6	4.0
CO	11	7.0	22	30	6.7	16	20
CH4	0.63	0.26	0.56	0.29	0.89	-	0.21
C2H6	1.7	1.5	4.9	4.9	14	2.0	1.4
H2S	0.17	1.7	7.9	8.0	51	0.35	2.5
SO2	13	33	41	26	92	154	19
N2	7.1	4.4	8.0	15	2.4	8.8	11
NH3	-	-	-	-	-	-	-

Gas Analyses of Copper Flat Mine Samples, continued

Sample	5-5	6-2	6-6	7-1	7-7	BX-1	fluid inclusion
Rock Type	qzmonz	and	qzmonz	and	and	bx	qz
Gas (X 10 ⁻⁷ moles)							
H ₂ O	780	56	830	390	670	1100	1200
H ₂	2.3	0.87	9.8	6.6	21	0.5	20
CO ₂	84	9.9	4.9	18	39	120	37
CO	51	12	14	18	81	48	1.1
CH ₄	1.5	0.92	0.45	0.67	3.2	1.3	0.4
C ₂ H ₆	-	1.5	1.7	2.9	9.4	-	-
H ₂ S	-	3.5	1.0	26	8.4	0.3	5.3
SO ₂	0.47	5.5	6.7	8.5	11	5.8	4.2
N ₂	2.3	7.0	5.4	25	-	-	-
NH ₃	-	-	-	-	-	-	-

Explanation: *=step-heated, - =not detected, bio=hydrothermal biotite, BIO=igneous biotite, chl=hydrothermal chlorite, CHL=metamorphic chlorite, ser=hydrothermal sericite, MUSC=igneous or metamorphic sericite and muscovite, and=andesite, bx=breccia, lat por=latite porphyry, monz=monzonite, qz=quartz, qzite=quartzite, qz lat=quartz latite, qz monz=quartz monzonite

This thesis is accepted on behalf of the faculty
of the Institute by the following committee:

David L. Nannon
Adviser

James M. Rector
Andrew R Campbell

Nov. 28 1983
Date